

1 **Title:**

2 **Global trait–environment relationships of plant communities**

3

4 **One Sentence Summary:** Trait composition of plant communities across the globe is  
5 captured by two main dimensions and is shaped predominantly by environmental filtering, but  
6 is only weakly related to global climate and soil gradients.

7 **Authors:**

8 Helge Bruelheide<sup>1,2</sup>, Jürgen Dengler<sup>2,3,4</sup>, Oliver Purschke<sup>1,2</sup>, Jonathan Lenoir<sup>5</sup>, Borja Jiménez-  
9 Alfaro<sup>1,2,6</sup>, Stephan M. Hennekens<sup>7</sup>, Zoltán Botta-Dukát<sup>8</sup>, Milan Chytrý<sup>6</sup>, Richard Field<sup>9</sup>,  
10 Florian Jansen<sup>10</sup>, Jens Kattge<sup>2,11</sup>, Valério D. Pillar<sup>12</sup>, Franziska Schrodtr<sup>9,11</sup>, Miguel D.  
11 Mahecha<sup>2,11</sup>, Robert K. Peet<sup>13</sup>, Brody Sandel<sup>14</sup>, Peter van Bodegom<sup>15</sup>, Jan Altman<sup>16</sup>, Esteban  
12 Alvarez Davila<sup>17</sup>, Mohammed A.S. Arfin Khan<sup>18,19</sup>, Fabio Attorre<sup>20</sup>, Isabelle Aubin<sup>21</sup>,  
13 Christopher Baraloto<sup>22</sup>, Jorcely G. Barroso<sup>23</sup>, Marijn Bauters<sup>24</sup>, Erwin Bergmeier<sup>25</sup>, Idoia  
14 Biurrun<sup>26</sup>, Anne D. Bjorkman<sup>27</sup>, Benjamin Blonder<sup>28,29</sup>, Andraž Čarni<sup>30,31</sup>, Luis Cayuela<sup>32</sup>,  
15 Tomáš Černý<sup>33</sup>, J. Hans C. Cornelissen<sup>34</sup>, Dylan Craven<sup>2,35</sup>, Matteo Dainese<sup>36</sup>, Géraldine  
16 Derroire<sup>37</sup>, Michele De Sanctis<sup>20</sup>, Sandra Díaz<sup>38</sup>, Jiří Doležal<sup>16</sup>, William Farfan-Rios<sup>39,40</sup>, Ted  
17 R. Feldpausch<sup>41</sup>, Nicole J. Fenton<sup>42</sup>, Eric Garnier<sup>43</sup>, Greg R. Guerin<sup>44</sup>, Alvaro G. Gutiérrez<sup>45</sup>,  
18 Sylvia Haider<sup>1,2</sup>, Tarek Hattab<sup>46</sup>, Greg Henry<sup>47</sup>, Bruno Hérault<sup>48,49</sup>, Pedro Higuchi<sup>50</sup>, Norbert  
19 Hölzel<sup>51</sup>, Jürgen Homeier<sup>52</sup>, Anke Jentsch<sup>19</sup>, Norbert Jürgens<sup>53</sup>, Zygmunt Kącki<sup>54</sup>, Dirk N.  
20 Karger<sup>55,56</sup>, Michael Kessler<sup>55</sup>, Michael Kleyer<sup>57</sup>, Ilona Knollová<sup>6</sup>, Andrey Y. Korolyuk<sup>58</sup>,  
21 Ingolf Kühn<sup>35,1,2</sup>, Daniel C. Laughlin<sup>59,60</sup>, Frederic Lens<sup>61</sup>, Jacqueline Loos<sup>62</sup>, Frédérique  
22 Louault<sup>63</sup>, Mariyana I. Lyubenova<sup>64</sup>, Yadvinder Malhi<sup>65</sup>, Corrado Marcenò<sup>26</sup>, Maurizio  
23 Mencuccini<sup>66,67</sup>, Jonas V. Müller<sup>68</sup>, Jérôme Munzinger<sup>69</sup>, Isla H. Myers-Smith<sup>70</sup>, David A.  
24 Neill<sup>71</sup>, Ülo Niinemets<sup>72</sup>, Kate H. Orwin<sup>73</sup>, Wim A. Ozinga<sup>7,74</sup>, Josep Penuelas<sup>67,72,75</sup>, Aaron  
25 Pérez-Haase<sup>76,77</sup>, Petr Petřík<sup>16</sup>, Oliver L. Phillips<sup>78</sup>, Meelis Pärtel<sup>79</sup>, Peter B. Reich<sup>80,81</sup>,  
26 Christine Römermann<sup>2,82</sup>, Arthur V. Rodrigues<sup>83</sup>, Jordi Sardans<sup>67,75</sup>, Marco Schmidt<sup>84</sup>, Gunnar  
27 Seidler<sup>1</sup>, Javier Eduardo Silva Espejo<sup>85</sup>, Marcos Silveira<sup>86</sup>, Anita Smyth<sup>44</sup>, Maria Sporbert<sup>1,2</sup>,  
28 Jens-Christian Svenning<sup>27</sup>, Raquel Thomas<sup>87</sup>, Ioannis Tsiripidis<sup>88</sup>, Kiril Vassilev<sup>89</sup>, Cyrille  
29 Violle<sup>43</sup>, Risto Virtanen<sup>2,90,91</sup>, Evan Weiher<sup>92</sup>, Erik Welk<sup>1,2</sup>, Karsten Wesche<sup>2,93,94</sup>, Marten  
30 Winter<sup>2</sup>, Christian Wirth<sup>2,11,95</sup>, Ute Jandt<sup>1,2</sup>

31 **Affiliations:**

32 <sup>1</sup> Martin Luther University Halle-Wittenberg, Institute of Biology/Geobotany and Botanical  
33 Garden, Am Kirchtor 1, 06108 Halle, Germany

34 <sup>2</sup> German Centre for Integrative Biodiversity Research (iDiv) Halle-Jena-Leipzig, Deutscher  
35 Platz 5e, 04103 Leipzig, Germany

36 <sup>3</sup> Zurich University of Applied Sciences (ZHAW), Institute of Natural Resource Sciences  
37 (IUNR), Research Group Vegetation Ecology, Grüentalstr. 14, Postfach, 8820 Wädenswil,  
38 Switzerland

39 <sup>4</sup> University of Bayreuth, Bayreuth Center of Ecology and Environmental Research  
40 BayCEER, Plant Ecology, Universitätsstr. 30, 95447 Bayreuth, Germany

41 <sup>5</sup> Université de Picardie Jules Verne, UR Ecologie et Dynamique des Systèmes Anthropisés  
42 (EDYSAN, FRE 3498 CNRS-UPJV), 1 rue des Louvels, 80037 Amiens Cedex 1, France

43 <sup>6</sup> Masaryk University, Department of Botany and Zoology, Kotlářská 2, 611 37 Brno, Czech  
44 Republic

45 <sup>7</sup> Wageningen Environmental Research (Alterra), Team Vegetation, Forest and Landscape  
46 Ecology, PO Box 47, 6700 AA Wageningen, The Netherlands

47 <sup>8</sup> MTA Centre for Ecological Research, GINOP Sustainable Ecosystems Group, 8237 Tihany,  
48 Klebesberg Kuno u. 3, Hungary

49 <sup>9</sup> University of Nottingham, School of Geography, University Park, Nottingham, NG7 2RD,  
50 United Kingdom

51 <sup>10</sup> University of Rostock, Faculty for Agricultural and Environmental Sciences, Justus-von-  
52 Liebig-Weg 6, 18059 Rostock, Germany

53 <sup>11</sup> Max Planck Institute for Biogeochemistry, Hans-Knöll-Str. 10, 07745 Jena, Germany

54 <sup>12</sup> Universidade Federal do Rio Grande do Sul, Department of Ecology, Porto Alegre, RS,  
55 91501-970, Brazil

56 <sup>13</sup> University of North Carolina at Chapel Hill, Department of Biology, Chapel Hill, NC  
57 27599-3280, USA

58 <sup>14</sup> Department of Biology, Santa Clara University, Santa Clara CA 95053, USA

59 <sup>15</sup> Leiden University, Institute of Environmental Sciences, Department Conservation Biology,  
60 Einsteinweg 2, 2333 CC Leiden, The Netherlands

61 <sup>16</sup> Institute of Botany of the Czech Academy of Sciences, Zámek 1, 252 43 Průhonice, Czech  
62 Republic

63 <sup>17</sup> Escuela de Ciencias Agropecuarias y Ambientales – ECAPMA, Universidad Nacional  
64 Abierta y a Distancia –UNAD, Sede José Celestino Mutis, Calle 14S #14, Bogotá

65 <sup>18</sup> Shahjalal University of Science and Technology, Department of Forestry and  
66 Environmental Science, Sylhet, 3114, Bangladesh

67 <sup>19</sup> University of Bayreuth, Bayreuth Center of Ecology and Environmental Research  
68 BayCEER, Department of Disturbance Ecology, Universitätsstr. 30, 95447 Bayreuth,  
69 Germany

70 <sup>20</sup> Sapienza University of Rome, Department of Environmental Biology, P.le Aldo Moro 5,  
71 00185 Rome, Italy

72 <sup>21</sup> Great Lakes Forestry Centre, Canadian Forest Service, Natural Resources Canada, 1219  
73 Queen St. East, Sault Ste Marie, ON, P6A 2E5, Canada

74 <sup>22</sup> Florida International University, Department of Biological Sciences, International Center  
75 for Tropical Botany (ICTB), 11200 SW 8th Street, OE 243 Miami, FL 33199, USA

76 <sup>23</sup> Universidade Federal do Acre, Campus de Cruzeiro do Sul, Acre, Brazil.

77 <sup>24</sup> Ghent University, Faculty of Bioscience Engineering, Department of Applied Analytical  
78 and Physical Chemistry, ISOFYS, Coupure Links 653, 9000 Gent, Belgium

79 <sup>25</sup> University of Göttingen, Albrecht von Haller Institute of Plant Sciences, Vegetation  
80 Analysis & Plant Diversity, Untere Karspüle 2, 37073 Göttingen, Germany

81 <sup>26</sup> University of the Basque Country UPV/EHU, Apdo. 644, 48080 Bilbao, Spain

82 <sup>27</sup> Aarhus University, Department of Bioscience, Section for Ecoinformatics & Biodiversity,  
83 Ny Munkegade 114, 8000 Aarhus C, Denmark

84 <sup>28</sup> University of Oxford, Environmental Change Institute, School of Geography and the  
85 Environment, South Parks Road, Oxford OX1 3QY, United Kingdom

86 <sup>29</sup> Rocky Mountain Biological Laboratory, PO Box 519, Crested Butte, Colorado, 81224 USA

87 <sup>30</sup> Scientific Research Center of the Slovenian Academy of Sciences and Arts, Institute of  
88 Biology, Novi trg 2, SI 1001 Ljubljana p. box 306, Slovenia

89 <sup>31</sup> University of Nova Gorica, 5000 Nova Gorica, Slovenia

90 <sup>32</sup> Universidad Rey Juan Carlos, Department of Biology, Geology, Physics and Inorganic  
91 Chemistry, c/ Tulipán s/n, 28933 Móstoles, Madrid, Spain

92 <sup>33</sup> Czech University of Life Sciences, Faculty of Forestry and Wood Science, Department of  
93 Forest Ecology, Kamýcká 1176, 16521, Praha 6 – Suchbát, Czech Republic

94 <sup>34</sup> Vrije Universiteit Amsterdam, Faculty of Science, Department of Ecological Science, De  
95 Boelelaan 1085, 1081 HV Amsterdam, The Netherlands

96 <sup>35</sup> Helmholtz Centre for Environmental Research - UFZ, Dept. Community Ecology,  
97 Theodor-Lieser-Str. 4, 06120 Halle, Germany

98 <sup>36</sup> University of Würzburg, Department of Animal Ecology and Tropical Biology, Am  
99 Hubland, 97074 Würzburg, Germany

100 <sup>37</sup> Cirad, UMR EcoFoG, Campus Agronomique, 97310 Kourou, French Guiana

101 <sup>38</sup> Universidad Nacional de Córdoba, Instituto Multidisciplinario de Biología Vegetal  
102 (IMBIV), CONICET and FCEfyN, Casilla de Correo 495, 5000 Córdoba, Argentina.

103 <sup>39</sup> Wake Forest University, Department of Biology, Winston Salem, North Carolina, USA

104 <sup>40</sup> Universidad Nacional de San Antonio Abad del Cusco, Herbario Vargas (CUZ), Cusco,  
105 Peru

106 <sup>41</sup> University of Exeter, College of Life and Environmental Sciences, Geography, Exeter, EX4  
107 4RJ, United Kingdom.

108 <sup>42</sup> Université du Québec en Abitibi-Témiscamingue, Institut de recherche sur les forêts, 445  
109 Boul. de l'Université, Rouyn-Noranda, Qc J9X 4E5, Canada

110 <sup>43</sup> CNRS - Université de Montpellier - Université Paul-Valéry Montpellier - EPHE, Centre  
111 d'Ecologie Fonctionnelle et Evolutive (UMR5175), 34293 Montpellier Cedex 5, France

112 <sup>44</sup> Terrestrial Ecosystem Research Network, School of Biological Sciences, University of  
113 Adelaide, Adelaide, South Australia, 5005 Australia

114 <sup>45</sup> Universidad de Chile, Facultad de Ciencias Agrónomas, Departamento de Ciencias  
115 Ambientales y Recursos Naturales Renovables, Av. Santa Rosa 11315, La Pintana 8820808,  
116 Santiago, Chile

117 <sup>46</sup> IFREMER (Institut Français de Recherche pour l'Exploitation de la MER) UMR 248  
118 MARBEC (CNRS, IFREMER, IRD, UM), 34203 Sète cedex, France

119 <sup>47</sup> University of British Columbia, The Department of Geography, 1984 West Mall,  
120 Vancouver, BC V6T 1Z2, Canada

121 <sup>48</sup> INPHB (Institut National Polytechnique Félix Houphouët-Boigny), BP 1093,  
122 Yamoussoukro, Ivory Coast

123 <sup>49</sup> Cirad, University Montpellier, UR Forests & Societies, Montpellier, France

124 <sup>50</sup> Universidade do Estado de Santa Catarina (UDESC), Departamento de Engenharia  
125 Florestal, Av Luiz de Camões, 2090 - Conta Dinheiro, Lages – SC, 88.520 – 000, Brazil

126 <sup>51</sup> University of Münster, Institute of Landscape Ecology, Heisenbergstr. 2, 48149 Münster,  
127 Germany

128 <sup>52</sup> University of Göttingen, Plant Ecology and Ecosystems Research, Untere Karaspüle 2,  
129 37073 Göttingen, Germany

130 <sup>53</sup> University of Hamburg, Biodiversity, Biocenter Klein Flottbek and Botanical Garden,  
131 Ohnhorststr. 18, 22609 Hamburg, Germany

132 <sup>54</sup> University of Wrocław, Institute of Environmental Biology, Department of Vegetation  
133 Ecology, Przybyszewskiego 63, 51-148 Wrocław, Poland

134 <sup>55</sup> University of Zurich, Department of Systematic and Evolutionary Botany, Zollikerstrasse  
135 107, 8008 Zurich, Switzerland

136 <sup>56</sup> Swiss Federal Research Institute WSL, Zürcherstrasse 111, 8903 Birmensdorf, Switzerland.

137 <sup>57</sup> University of Oldenburg, Institute of Biology and Environmental Sciences, Landscape  
138 Ecology Group, Carl-von-Ossietzky Strasse 9-11, 26111 Oldenburg, Germany

139 <sup>58</sup> Central Siberian Botanical Garden SB RAS, Zolotodolinskaya str. 101, Novosibirsk,  
140 630090, Russia

141 <sup>59</sup> Environmental Research Institute, School of Science, University of Waikato, Private Bag  
142 3105, Hamilton 3240, New Zealand

143 <sup>60</sup> University of Wyoming, Department of Botany, Laramie, Wyoming, USA

144 <sup>61</sup> Naturalis Biodiversity Center, Leiden University, P.O. Box 9517, 2300RA Leiden, The  
145 Netherlands

146 <sup>62</sup> Agroecology, University of Göttingen, Grisebachstrasse 6, 37077 Göttingen, Germany

147 <sup>63</sup> INRA, VetAgro Sup, UMR Ecosystème Prairial, 63000 Clermont-Ferrand, France

148 <sup>64</sup> University of Sofia, Faculty of Biology, Department of Ecology and Environmental  
149 Protection, 1164 Sofia, 8 Dragan Tsankov Av., Bulgaria

150 <sup>65</sup> University of Oxford, Environmental Change Institute, School of Geography and the  
151 Environment, South Parks Road, Oxford, OX1 3QY, United Kingdom

152 <sup>66</sup> ICREA Pg. Lluís Companys 23, 08010 Barcelona, Spain

153 <sup>67</sup> CREAM, Cerdanyola del Vallès, 08193 Barcelona, Catalonia, Spain

154 <sup>68</sup> Royal Botanic Gardens Kew, Millennium Seed Bank, Conservation Science, Wakehurst  
155 Place, Ardingly, RH17 6TN, United Kingdom

156 <sup>69</sup> AMAP, IRD, CNRS, INRA, Université Montpellier, 34000 Montpellier, France

157 <sup>70</sup> University of Edinburgh, School of GeoSciences, Edinburgh EH9 3FF, United Kingdom

158 <sup>71</sup> Universidad Estatal Amazónica, Conservación y Manejo de Vida Silvestre, Paso lateral km  
159 2½ via a Napo Puyo, Pastaza, Ecuador

160 <sup>72</sup> Estonian University of Life Science, Department of Crop Science and Plant Biology,  
161 Kreutzwaldi 1, 51014, Tartu, Estonia

162 <sup>73</sup> Landcare Research, PO Box 69040, Lincoln 7640, New Zealand

163 <sup>74</sup> Institute for Water and Wetland Research, Radboud University Nijmegen, 6500 GL  
164 Nijmegen, The Netherlands

165 <sup>75</sup> CSIC, Global Ecology Unit, CREAM-CEAB-UAB, Cerdanyola del Vallès, 08193  
166 Barcelona, Catalonia, Spain

167 <sup>76</sup> University of Barcelona, Faculty of Biology, Department of Evolutionary Biology, Ecology  
168 and Environmental Sciences, Av. Diagonal 643, 08028, Barcelona, Spain

169 <sup>77</sup> Center for Advanced Studies of Blanes, Spanish Research Council  
170 (CEAB-CSIC), E-17300 Blanes, Spain

171 <sup>78</sup> University of Leeds, School of Geography, Leeds LS2 9JT, United Kingdom  
172 <sup>79</sup> University of Tartu, Ülikooli 18, 50090 Tartu, Estonia  
173 <sup>80</sup> University of Minnesota, Department of Forest Recourses, 220F Green Hall,  
174 1530 Cleveland Avenue North, St. Paul, MN 55108, USA  
175 <sup>81</sup> Hawkesbury Institute for the Environment, Western Sydney University, New South Wales 2751,  
176 Australia  
177 <sup>82</sup> Friedrich Schiller University Jena, Institute of Systematic Botany, Philosophenweg 16,  
178 07743 Jena, Germany  
179 <sup>83</sup> Universidade Regional de Blumenau, Departamento de Engenharia Florestal, Rua São  
180 Paulo, 3250, 89030-000 Blumenau-Santa Catarina, Brazil  
181 <sup>84</sup> Senckenberg Biodiversity and Climate Research Centre (BiK-F), Data and Modelling  
182 Centre, Senckenberganlage 25, 60325 Frankfurt am Main, Germany  
183 <sup>85</sup> University of La Serena , Department of Biology, La Serena, Chile  
184 <sup>86</sup> Universidade Federal do Acre, Museu Universitário / Centro de Ciências Biológicas e da  
185 Natureza / Laboratório de Botânica e Ecologia Vegetal, BR 364, Km 04 - Distrito Industrial -  
186 69915-559 - Rio Branco-AC, Brazil  
187 <sup>87</sup> Iwokrama International Centre for Rain Forest Conservation and Development, 77 High  
188 Street, Kingston, Georgetown, Guyana  
189 <sup>88</sup> Aristotle University of Thessaloniki, School of Biology, Department of Botany, 54124  
190 Greece  
191 <sup>89</sup> Bulgarian Academy of Sciences, Institute of Biodiversity and Ecosystem Research, 23  
192 Acad. G. Bonchev Str., 1113 Sofia, Bulgaria  
193 <sup>90</sup> Helmholtz Center for Environmental Research – UFZ, Department of Physiological  
194 Diversity, Permoserstraße 15, Leipzig 04318, Germany  
195 <sup>91</sup> University of Oulu, Department of Ecology & Genetics, PO Box 3000, FI-90014, Finland  
196 <sup>92</sup> University of Wisconsin - Eau Claire, Department of Biology, Eau Claire, WI 54702-4004,  
197 USA  
198 <sup>93</sup> Senckenberg Museum of Natural History Görlitz, P.O. Box 300154, 02806 Görlitz,  
199 Germany  
200 <sup>94</sup> TU Dresden, International Institute (IHI) Zittau, Markt 23, 02763 Zittau, Germany  
201 <sup>95</sup> University of Leipzig, Systematic Botany and Functional Biodiversity, Johannisallee 21-23,  
202 04103 Leipzig, Germany  
203

204 **Abstract:**

205 Plant functional traits directly affect ecosystem functions and are fundamental for managing  
206 and predicting biodiversity and ecosystem change. Globally, at the species level, plant trait  
207 combinations depend on key trade-offs representing different ecological strategies<sup>1</sup>, but at the  
208 community level trait combinations may be decoupled from these trade-offs because different  
209 strategies can facilitate co-existence within communities<sup>2</sup>. A key remaining question is to  
210 what extent community-level trait composition depends on local factors (microclimate, fine-  
211 scale soil properties, disturbance regime<sup>3</sup>, successional dynamics<sup>4</sup>) and regional to global  
212 environmental drivers (macroclimate<sup>5-7</sup>, coarse-scale soil properties<sup>8,9</sup>). Here, we perform the  
213 first global, plot-level analysis of trait-environment relationships, using a novel database with  
214 more than 1.1 million vegetation plots and 26,632 plant species with trait information. We  
215 show that the two main community trait axes (plant stature and resource acquisitiveness),  
216 which capture half of the global trait variation, are weakly associated with climate and soil  
217 conditions at the global scale. Thus, similar climate and soil conditions support communities  
218 differing greatly in mean trait values, and within-plot trait variation does not vary  
219 systematically with macro-environment. Beyond the two main trait dimensions, we found a  
220 strong correlation between leaf N:P ratio and growing-season warmth, indicating increasing  
221 phosphorus limitation towards the tropics. Our results indicate that, at fine grains, macro-  
222 environmental drivers are much less important for functional trait composition than has  
223 hitherto been assumed from analyses restricted to co-occurrence in large grid cells. Instead,  
224 trait combinations may predominantly reflect local-scale factors such as disturbance, fine-  
225 scale soil conditions, niche partitioning or biotic interactions.

226

227 **Main Text:**

228 How climate drives the functional characteristics of vegetation across the globe has been a  
229 key question in ecological research for more than a century<sup>10</sup>. While functional information is  
230 available for a large portion of the global pool of plant species, we do not know how  
231 functional traits of co-occurring species are combined, which is what determines their joint  
232 effect on ecosystems<sup>4,8,11</sup>. At the species level, Díaz et al.<sup>1</sup> demonstrated that 74% of the  
233 global spectrum of six key plant traits determining plant fitness in terms of survival, growth  
234 and reproduction can be accounted for by two principal components (PCs). They showed that  
235 the functional space occupied by vascular plant species is strongly constrained by trade-offs  
236 between traits and converges on a small set of successful trait combinations, confirming  
237 previous findings<sup>7,12-14</sup>. While these constraints describe evolutionarily viable ecological  
238 strategies for vascular plant species globally, they provide only limited insight into trait  
239 composition within communities. This is information necessary to understand how climate  
240 change and other anthropogenic drivers affect ecosystem functioning at the global scale.

241 So far, studies relating trait composition to the environment at continental to global extents  
242 have been restricted to coarse-grained species occurrence data (e.g. presence in 1° grid cells<sup>15-  
243 17</sup>). Such data capture neither biotic interactions (co-occurrence in large grid cells does not  
244 indicate local co-existence), nor local variation in environmental filters (e.g. variation in soil,

245 topography or disturbance regime within grid cells). In contrast, functional composition  
246 within vegetation plots with sizes of a few hundred square meters is the direct outcome of  
247 these local factors. Here, we present the first global analysis of plot-level trait composition.  
248 We combined the ‘sPlot’ database, a new global initiative incorporating more than 1.1 million  
249 vegetation plots from over 100 databases (mainly forests and grasslands; see Methods), with  
250 30 large-scale environmental variables and 18 key plant functional traits derived from TRY, a  
251 global plant-trait database (see Methods, Table 1, Extended Data Table 1).

252 We used this unprecedented fine-resolution worldwide dataset to test the hypothesis  
253 (Hypothesis 1) that environmental filtering is the main global structuring force of community  
254 trait composition. Globally, temperature and precipitation drive the differences in vegetation  
255 between biomes, suggesting strong environmental filtering<sup>3,8</sup> that constrains the number of  
256 successful trait combinations and leads to community-level trait convergence. Trait  
257 convergence also results from other mechanisms (biotic interactions may eliminate  
258 excessively divergent trait combinations<sup>18,19</sup>), and alternative functional trait combinations  
259 may confer equal fitness in the same environment<sup>2</sup>. Thus, stronger environmental filtering is  
260 expected to result in both greater global variation of plot-level trait means, and less trait  
261 variation within plots, than expected by chance. Furthermore, with strong trait convergence,  
262 trait spectra of plant communities should mirror those of individual species<sup>1</sup>.

263 The main environmental drivers of this filtering should correlate strongly (though not  
264 necessarily linearly<sup>20</sup>) with plot-level trait means and with within-plot trait variance.  
265 Identifying these drivers has the potential to fundamentally alter our understanding of global  
266 trait-environment relationships. We tested the hypothesis (Hypothesis 2) that there are strong  
267 correlations with respect to global environmental drivers such as macroclimate and coarse-  
268 scale soil properties<sup>5-9,15-17,20-24</sup> (see Table 1 for expected relationships and Extended Data  
269 Table 2 for variables used).

270 Consistent with hypothesis 1, global variation in plot-level trait means was much higher than  
271 expected by chance: all traits had positive standardized effect sizes (SEs), which were  
272 significantly  $> 0$  for 17 out of 18 traits (mean SES = 8.06 standard deviations (SD), Extended  
273 Data Table 1). This suggests that environmental filtering is the prevailing force of community  
274 trait composition globally. Also confirming hypothesis 1, within-plot trait variance was  
275 typically lower than expected by chance (mean SES = -1.76 SD, significantly  $< 0$  for ten traits  
276 but significantly  $> 0$  for three traits; Extended Data Table 1). Thus, global environmental  
277 filtering may also constrain trait variation within communities.

278 Trait correlations at the community level were relatively well captured by the first two axes of  
279 a Principal Component Analysis (PCA) for both plot-level trait means and within-plot trait  
280 variances (Figures 1 and 2). The dominant axes were determined by those traits with the  
281 highest absolute SEs of mean trait values (Extended Data Table 1). The PCA of plot-level  
282 trait means (Fig. 1) reflects two main functional continua on which community trait values  
283 converge: one from short-stature, small-seeded communities such as grasslands or herbaceous  
284 vegetation to tall-stature communities with large, heavy diaspores such as forests (the size  
285 spectrum), and the other from communities with resource acquisitive to those with resource  
286 conservative leaves (i.e. the leaf economics spectrum)<sup>12</sup>. The high similarity between this



287 PCA and the one at the species level by Díaz et al.<sup>1</sup> is striking: here at the community level,  
288 based on 1.1 million plots, the same functional continua emerged as at the species level, based  
289 on 2,214 species, revealing a strong parallel of present-day community assembly to individual  
290 species' evolutionary histories. This strong congruence between community-level and  
291 species-level trait spectra also corroborates our finding of strong trait convergence.

292 Surprisingly, we found only limited support for our second hypothesis. Community-level trait  
293 composition was poorly captured by global climate and soil variables. None of the 30  
294 environmental variables accounted individually for more than 10% of the variance in the traits  
295 defining the main dimensions in Fig. 1 (Extended Data Fig. 1). The coefficients of  
296 determination were not improved when testing for non-linear relationships (see Methods).  
297 Using all 30 environmental variables simultaneously as predictors only accounted for 10.8%  
298 or 14.0% of the overall variation in plot-level trait means (cumulative variance, respectively,  
299 of the first two or all 18 constrained axes in a Redundancy Analysis). Overall, our results  
300 show that similar global-scale climate and soil conditions can support communities that differ  
301 markedly in mean trait values and that different climates can support communities with rather  
302 similar mean trait values.

303 The ordination of within-plot variance of the different traits (Fig. 2) revealed two main  
304 continua. Variances of plant height and diaspore mass varied largely independently of  
305 variances of traits representing the leaf economics spectrum. These results suggest that short  
306 and tall species can be assembled together in the same community independently from  
307 combining species with acquisitive leaves together with species with conservative leaves.  
308 Global climate and soil variables accounted for even less variation on the first two PCA axes  
309 in within-plot trait variances than on the first two PCA axes in plot-level trait means. Only  
310 two environmental variables had  $r^2 > 3\%$  (Extended Data Fig. 2), whether allowing for non-  
311 linear relationships (see Methods) or not, and overall, macro-environment accounted for only  
312 3.6% or 5.0% of the variation (cumulative variance, respectively, of the first two or all 18  
313 constrained axes). Removing species richness effects from within-plot trait variances did not  
314 increase the amount of variation explained by the environment (see Methods).

315 These results suggest that plot-level trait means and variation may both be predominantly  
316 driven by local environmental factors, such as topography (e.g. north- vs. south-facing  
317 slopes), local soil characteristics (e.g. soil depth and nutrient supply)<sup>8,9,24,25</sup>, disturbance  
318 regime (including land use<sup>26</sup> and successional status<sup>4,27</sup>) or biotic interactions<sup>18-19</sup>. These  
319 findings contrast strongly with studies where the variation in traits between species was  
320 calculated at the level of the species pool in large grid cells<sup>15,16</sup>, demonstrating that plot-level  
321 and grid cell-level trait composition are driven by different factors<sup>21</sup>.

322 The strongest community-level correlations with environment were found for traits that were  
323 not linked to the leaf economics spectrum. Mean stem specific density increased with  
324 potential evapotranspiration (PET,  $r^2=15.6\%$ ; Fig. 3a, b), reflecting the need to produce  
325 denser wood with increasing evaporative demand. Leaf N:P ratio increased with growing-  
326 season warmth (growing degree days above 5°C, GDD5,  $r^2=11.5\%$ ; Fig. 3d), indicating strong  
327 phosphorus limitation<sup>28</sup> in most of the southern hemisphere (Fig. 3c, d). This pattern was not  
328 brought about by a parallel increase in the presence of legumes, which tend to have relatively

329 high N:P ratios; excluding all species of Fabaceae resulted in a very similar relationship with  
330 GDD5 ( $r^2=10.0\%$ ). The global N:P pattern is consistent with results based on traits of single  
331 species related to mean annual temperature<sup>29</sup>. The underlying mechanism is the high soil  
332 weathering rate at high temperatures and humidity, which in the southern hemisphere was not  
333 reset by glaciation. We propose that phosphorus limitation may weaken the relationships  
334 between productivity-related traits and macroclimate (Extended Data Fig. 2). For example,  
335 specific leaf area may be similarly affected by low nutrient availability<sup>8-9,24-25</sup> in favourable  
336 climates as by low temperature and precipitation under favourable nutrient supply. Overall,  
337 our findings are relevant in improving Dynamic Global Vegetation Models (DGVMs), which  
338 so far have used trait information only from a few calibration plots<sup>22</sup>. The sPlot database  
339 provides much-needed empirical data on the community trait pool in DGVMs<sup>30</sup> and identifies  
340 traits that should be considered when predicting vegetation, such as stem specific density and  
341 leaf N:P ratio.

342 We also assessed whether the observed trait-environment relationships hold for forests and  
343 non-forest vegetation independently (see Methods). Both subsets confirmed the overall  
344 patterns in trait means (Extended Data Figs. 3-6). The variance in plot-level trait means  
345 explained by large-scale climate and soil variables was higher for forest than non-forest plots,  
346 probably because forests belong to a well-defined and rather resource-conservative formation,  
347 whereas non-forest plots encompass a heterogeneous mixture of different vegetation types,  
348 ranging from alpine meadows to semi-deserts, and tend to depend more on disturbance and  
349 management, which can strongly affect trait-environment relationships of communities<sup>21</sup>. We  
350 also tested whether our findings depended on the uneven distribution of plots among the  
351 world's different climates and soils and repeated the analyses in 100 subsets of ~100,000 plots  
352 resampled in the global climate space (Extended Data Figs. 7-8). The analyses of the  
353 resampled datasets revealed the same patterns, but more strongly, and confirmed the impact of  
354 PET and GDD5 on stem specific density and leaf N:P ratio, respectively. The correlations  
355 between trait means and environmental variables were stronger in the resampled subsets  
356 because the resampling procedure significantly reduced the overrepresentation of the  
357 temperate-zone areas with intermediate climatic values.

358 Our findings have important implications for understanding and predicting plant community  
359 trait assembly. First, worldwide trait variation of plant communities is captured by a few main  
360 dimensions of variation that are consistent with species-based studies<sup>1,12-14</sup>, suggesting that the  
361 drivers of past trait evolution, which resulted in the present-day species-level trait spectra<sup>1</sup>, are  
362 also reflected in the composition of today's plant communities. If species-level trade-offs  
363 indeed constrain community assembly, then the present-day contrasts in trait composition of  
364 terrestrial plant communities should also have existed in the past and will probably remain,  
365 even for novel communities, in the future. Second, clear plot-level vegetation trait continua  
366 cannot easily be captured by coarse-resolution environmental variables<sup>21</sup>. This brings into  
367 question both the use of simple large-scale climate relationships to predict the leaf economics  
368 spectra of global vegetation<sup>6,15-16,22</sup> and attempts to derive net primary productivity and global  
369 carbon and water budgets from global climate, even when employing powerful trait-based  
370 vegetation models<sup>30</sup>. The finding that within-plot trait variances were only very weakly  
371 related to global climate or soil variables points to the importance of either local-scale climate

372 or soil variables or to disturbance regimes for the degree of local trait dispersion<sup>3</sup>. Finally,  
373 both the limited role of large-scale climate in explaining trait patterns and the relevance of  
374 phosphorus limitation call for including local variables when predicting community trait  
375 patterns. At the same place in global climate space, communities can vary greatly in trait  
376 means and variances, consistent with high local variation in species' trait values<sup>7-8,12</sup>. Future  
377 research on functional response of communities to changing climate should incorporate the  
378 effect of local environmental conditions<sup>24-26</sup> and biotic interactions<sup>18-19</sup> for building reliable  
379 predictions of vegetation dynamics.

380

## 381 **References**

- 382 1. Díaz, S. *et al.* The global spectrum of plant form and function. *Nature* **529**, 167-171 (2016).
- 383 2. Marks, C.O. & Lechowicz, M.J. Alternative designs and the evolution of functional  
384 diversity. *Am. Nat.* **167**, 55–67 (2006).
- 385 3. Grime, J.P. Trait convergence and trait divergence in herbaceous plant communities:  
386 Mechanisms and consequences. *J. Veg. Sci.* **17**, 255–260 (2006).
- 387 4. Garnier, E. *et al.* Plant functional markers capture ecosystem properties during secondary  
388 succession. *Ecology* **85**, 2630–2637 (2004).
- 389 5. Muscarella, R. & Uriarte, M. Do community-weighted mean functional traits reflect  
390 optimal strategies? *Proc. R. Soc. B.* **283**, 20152434 (2016).
- 391 6. Swenson, N.G. & Weiser, M.D. Plant geography upon the basis of functional traits: An  
392 example from eastern North American trees. *Ecology* **91**, 2234–2241 (2010).
- 393 7. Moles, A.T. *et al.* Global patterns in plant height. *J. Ecol.* **97**, 923-932 (2009).
- 394 8. Ordoñez, J.C. *et al.* A global study of relationships between leaf traits, climate and soil  
395 measures of nutrient fertility. *Global Ecol. Biogeogr.* **18**, 137–149 (2009).
- 396 9. Fyllas, N.M. *et al.* Basin-wide variations in foliar properties of Amazonian forest:  
397 phylogeny, soils and climate. *Biogeosciences* **6**, 2677-2708 (2009).
- 398 10. Warming, E. *Lehrbuch der ökologischen Pflanzengeographie - Eine Einführung in die*  
399 *Kenntnis der Pflanzenvereine.* (Borntraeger, Berlin, 1896).
- 400 11. Garnier, E., Navas, M.-L. & Grigulis, K. *Plant functional diversity - Organism traits,*  
401 *community structure, and ecosystem properties.* (Oxford Univ. Press, 2016).
- 402 12. Wright, I.J. *et al.* The worldwide leaf economics spectrum. *Nature* **428**, 821-827 (2004).
- 403 13. Reich, P.B. The world-wide 'fast-slow' plant economics spectrum: a traits manifesto. *J.*  
404 *Ecol.* **102**, 275–301 (2014).

- 405 14. Adler, P.B. *et al.* Functional traits explain variation in plant life history strategies. *Proc.*  
406 *Natl. Acad. Sci. USA* **111**, 740–745 (2014).
- 407 15. Swenson, N.G. *et al.* Phylogeny and the prediction of tree functional diversity across  
408 novel continental settings. *Global Ecol. Biogeogr.* **26**, 553–562 (2017).
- 409 16. Swenson, N.G. *et al.* The biogeography and filtering of woody plant functional diversity  
410 in North and South America. *Global Ecol. Biogeogr.* **21**, 798–808 (2012).
- 411 17. Wright, I.J. *et al.* Global climatic drivers of leaf size. *Science* **357**: 917–921 (2017).
- 412 18. Mayfield, M.M. & Levine, J.M. Opposing effects of competitive exclusion on the  
413 phylogenetic structure of communities. *Ecol. Lett.* **13**, 1085 – 1093 (2010).
- 414 19. Kraft, N.J.B. *et al.* Community assembly, coexistence and the environmental filtering  
415 metaphor. *Funct. Ecol.* **29**, 592–599 (2015).
- 416 20. Barboni, D. *et al.* Relationships between plant traits and climate in the Mediterranean  
417 region: A pollen data analysis. *J. Veg. Sci.* **15**, 635-646 (2004).
- 418 21. Borgy, B. *et al.* Plant community structure and nitrogen inputs modulate the climate signal  
419 on leaf traits. *Global Ecol. Biogeogr.* **26**, 1138-1152 (2017).
- 420 22. van Bodegom, P.M, Douma, J.C. & Verheijen, L.M. A fully traits-based approach to  
421 modeling global vegetation distribution. *Proc. Natl. Acad. Sci. USA* **111**, 13733–13738  
422 (2014).
- 423 23. Moles, A.T. *et al.* Which is a better predictor of plant traits: Temperature or precipitation?  
424 *J. Veg. Sci.* **25**, 1167–1180 (2014).
- 425 24. Ordoñez, J.C. *et al.* Plant strategies in relation to resource supply in mesic to wet  
426 environments: Does theory mirror nature? *Am. Nat.* **175**, 225–239 (2010).
- 427 25. Simpson, A.J., Richardson, S.J. & Laughlin, D.C. Soil–climate interactions explain  
428 variation in foliar, stem, root and reproductive traits across temperate forests. *Global Ecol.*  
429 *Biogeogr.* **25**, 964-978 (2016).
- 430 26. Lienin, P. & Kleyer, M. Plant leaf economics and reproductive investment are responsive  
431 to gradients of land use intensity. *Agric. Ecosyst. Environ.* **145**, 67-76 (2011).
- 432 27. Maire, V. *et al.* Habitat filtering and niche differentiation jointly explain species relative  
433 abundance within grassland communities along fertility and disturbance gradients. *New*  
434 *Phytol.* **196**, 497–509 (2012).
- 435 28. Güsewell, S. N:P ratios in terrestrial plants: variation and functional significance. *New*  
436 *Phytol.* **164**, 243–266 (2004).
- 437 29. Reich, P.B. & Oleksyn, J. Global patterns of plant leaf N and P in relation to temperature  
438 and latitude, *Proc. Natl. Acad. Sci. USA* **101**, 11001-11006 (2004).

439 30. Scheiter, S., Langan, L. & Higgins, S.I. Next generation dynamic global vegetation  
440 models: learning from community ecology. *New Phytol.* **198**, 957-969 (2013).

441

442

#### 443 **Contributions**

444 H.B. and U.J. wrote the first draft of the manuscript, with considerable input by B.J.-A. and  
445 R.F.; H.B. carried out most of the statistical analyses and produced the graphs; H.B., O.Pu.  
446 and U.J. initiated sPlot as an sDiv working group and iDiv platform; J.De. compiled the plot  
447 databases globally; J.De., S.M.H., U.J., O.Pu. and F.J. harmonized vegetation databases; J.De.  
448 and B.J.-A. coordinated the sPlot consortium; J.K. provided the trait data from TRY; O.Pu.  
449 produced the taxonomic backbone; B.J.-A., G.S. and E. Welk compiled environmental data  
450 and produced the global maps; S.M.H. wrote the Turboveg v3 software, which holds the sPlot  
451 database; J.L. and T.H. wrote the resampling algorithm. Many authors participated in one or  
452 more of the three sPlot workshops at iDiv where the sPlot initiative was conceived and  
453 planned, and evaluation of the data and first drafts were discussed. All other authors  
454 contributed data. All authors contributed to writing the manuscript.

#### 455 **Acknowledgements**

456 sPlot has been initiated by sDiv, the Synthesis Centre of the German Centre for Integrative  
457 Biodiversity Research (iDiv) Halle-Jena-Leipzig, funded by the German Research Foundation  
458 (FZT 118) and now is a platform of iDiv. H.B., J.De., O.Pu, B.J.-A., J.K., D.C., M.W. and  
459 C.W. appreciate direct funding through iDiv. For all further acknowledgements see the  
460 Electronic Appendix.

## 461 **Material and Methods**

462 **Vegetation Data.** The sPlot 2.1 vegetation database contains 1,121,244 plots with 23,586,216  
463 species × plot observations, i.e. records of a species in a plot  
464 ([https://www.idiv.de/en/sdiv/working\\_groups/wg\\_pool/splot.html](https://www.idiv.de/en/sdiv/working_groups/wg_pool/splot.html)). This database aims at  
465 compiling plot-based vegetation data from all vegetation types worldwide, but with a  
466 particular focus on forest and grassland vegetation. Although the initial aim of sPlot was to  
467 achieve global coverage, the plots are very unevenly distributed with most data coming from  
468 Europe, North America and Australia and an overrepresentation of temperate vegetation types  
469 (Fig. 3).

470 For most plots (97.2%) information on species relative abundance was available, expressed as  
471 cover, basal area, individual count, importance value or per cent frequency in subplots. For  
472 the other 2.8% (31,461 plots), for which only presence/absence (p/a) was available, we  
473 assigned equal relative abundance to the species (1/species richness). For plots with a mix of  
474 cover and p/a information (mostly forest plots, where herb layer information had been added  
475 on a p/a basis; 8,524 plots), relative abundance was calculated by assigning the smallest cover  
476 value that occurred in a particular plot to all species with only p/a information in that plot.  
477 After removing plots without geographic coordinates and all observations on bryophytes and  
478 lichens, the database contained 22,195,966 observations on the relative abundance of vascular  
479 plant species in a total of 1,117,369 plots.

480 **Taxonomy.** To standardize the nomenclature of species within and between sPlot and TRY  
481 (see below), we constructed a taxonomic backbone of the 121,861 names contained in the two  
482 databases. Prior to name matching, we ran a series of string manipulation routines in R, to  
483 remove special characters and numbers, as well as standardized abbreviations in names.  
484 Taxon names were parsed and resolved using Taxonomic Name Resolution Service version  
485 4.0 (TNRS<sup>31</sup>; <http://tnrs.iplantcollaborative.org>; accessed 20 Sep 2015), selecting the best  
486 match across the five following sources: i) The Plant List (version 1.1;  
487 <http://www.theplantlist.org/>; Accessed 19 Aug 2015), ii) Global Compositae Checklist (GCC,  
488 <http://compositae.landcareresearch.co.nz/Default.aspx>; accessed 21 Aug 2015), iii)  
489 International Legume Database and Information Service (ILDIS,  
490 <http://www.ildis.org/LegumeWeb>; accessed 21 Aug 2015), iv) Tropicos  
491 (<http://www.tropicos.org/>; accessed 19 Dec 2014), and v) [USDA Plants Database](http://usda.gov/wps/portal/usda/usdahome)  
492 (<http://usda.gov/wps/portal/usda/usdahome>; accessed 17 Jan 2015). We allowed for partial  
493 matching to the next higher taxonomic rank (genus or family) in cases where full taxon names  
494 could not be found. All names matched or converted from a synonym by TNRS were  
495 considered accepted taxon names. In cases when no exact match was found (e.g. when  
496 alternative spelling corrections were reported), names with probabilities of  $\geq 95\%$  or higher  
497 were accepted and those with  $< 95\%$  were examined individually. Remaining non-matching  
498 names were resolved based on the National Center for Biotechnology Information's  
499 Taxonomy database (NCBI, <http://www.ncbi.nlm.nih.gov/>; accessed 25 Oct 2011) within  
500 TNRS, or sequentially compared directly against The Plant List and Tropicos (accessed  
501 September 2015). Names that could not be resolved against any of these lists were left as  
502 blanks in the final standardized name field. This resulted in a total of 86,760 resolved names,  
503 corresponding to 664 families, occurring in sPlot or TRY or both. Classification into families

504 was carried out according to APGIII<sup>32</sup>, and was used to identify non-vascular plant species  
505 (~5.1% of the taxon names) which were excluded from the subsequent statistical analysis.

506 **Trait Data.** Data for 18 traits that are ecologically relevant (Table 1) and sufficiently covered  
507 across species<sup>33</sup> were requested from TRY<sup>34</sup> (version 3.0) on the 10<sup>th</sup> August, 2016. We  
508 applied gap-filling with Bayesian Hierarchical Probabilistic Matrix Factorization  
509 (BHPMF<sup>33,35-36</sup>). We used the prediction uncertainties provided by BHPMF for each  
510 imputation to assess the quality of gap-filling and removed all imputations with a coefficient  
511 of variation > 1<sup>36</sup>. We obtained 18 gap-filled traits for 26,632 out of a total of 58,065 taxa in  
512 sPlot, which corresponds to 45.9% of all species but to 88.7% of all species × plot  
513 combinations. Trait coverage of the most frequent species was 77.2% and 96.2% for taxa that  
514 occurred in more than 100 or 1,000 plots, respectively. The gap-filled trait data comprised  
515 observed and imputed values on 632,938 individual plants, which we log<sub>e</sub> transformed and  
516 aggregated by taxon. For those taxa that were recorded at the genus level only, we calculated  
517 genus means. Out of 22,195,966 records of vascular plant species with geographic reference,  
518 21,172,989 (=95.4%) refer to taxa for which we had gap-filled trait values. This resulted in  
519 1,115,785 and 1,099,463 plots for which we had at least one taxon or two taxa with a trait  
520 value (99.5% and 98.1%, respectively, of the 1,121,244 plots that had vascular plants), and for  
521 which trait means and variances could be calculated.

522 We are aware that using species mean values for traits excludes the possibility to account for  
523 intraspecific variance, which can also strongly respond to the environment<sup>37</sup>. Thus, using one  
524 single value for a species is a source of error in calculating trait means and variances. In  
525 addition, some mean values of traits in TRY were based on a very small number of replicates  
526 per species, resulting in greater uncertainty in trait mean and variance calculations<sup>38</sup>.

527

528 **Environmental Data.** We compiled 30 environmental variables (Extended Data Table 2).  
529 Macroclimate variables were extracted from CHELSA<sup>39-40</sup>, V1.1 (Climatologies at High  
530 Resolution for the Earth's Land Surface Areas, [www.chelsa-climate.org](http://www.chelsa-climate.org)). CHELSA provides  
531 19 bioclimatic variables equivalent to those used in WorldClim ([www.worldclim.org](http://www.worldclim.org)) at a  
532 resolution of 30 arc sec (~ 1 km at the equator), averaging global climatic data from the  
533 period 1979-2013 and using a quasi-mechanistic statistical downscaling of the ERA-Interim  
534 reanalysis<sup>41</sup>.

535 Variables reflecting growing-season warmth were growing degree days above 1°C (GDD1)  
536 and 5°C (GDD5), calculated from CHELSA data<sup>42</sup>. We also compiled an index of aridity  
537 (AR) and a model for potential evapotranspiration (PET) extracted from the Consortium of  
538 Spatial Information (CGIAR-CSI) website ([www.cgiar-csi.org](http://www.cgiar-csi.org)). In addition, seven soil  
539 variables were extracted from the SOILGRIDS project (<https://soilgrids.org/>, licensed by  
540 ISRIC – World Soil Information), downloaded at 250 m resolution and then resampled using  
541 the 30 arc second grid of CHELSA (Extended Data Table 2). We refer to these climate and  
542 soil data as “environmental data”.

543 **Community trait composition.**

544 For every trait  $j$  and plot  $k$ , we calculated the plot-level trait means as community-weighted  
545 mean (CWM) according to<sup>4,43</sup>:

$$CWM_{j,k} = \sum_i^{n_k} p_{i,k} t_{i,j}$$

546 where  $n_k$  is the number of species sampled in plot  $k$ ,  $p_{i,k}$  is the relative abundance of species  $i$   
547 in plot  $k$ , referring to the sum of abundances for all species with traits in the plot, and  $t_{i,j}$  is the  
548 mean value of species  $i$  for trait  $j$ . This computation was done for each of the 18 traits for  
549 1,115,785 plots. The within-plot trait variance is given by community-weighted variance  
550 (CWV)<sup>43,44</sup>.

$$CWV_{j,k} = \sum_i^{n_k} p_{i,k} (t_{i,j} - CWM_{j,k})^2$$

551 CWV is equal to functional dispersion as described by Rao's quadratic entropy<sup>45</sup>, when using  
552 a squared Euclidean distance matrix  $d_{i,j,k}$ <sup>46</sup>:

$$CWV_{j,k} = \sum_i^{n_k} p_{i,k} (t_{i,j} - CWM_{j,k})^2 = FD_Q = \sum_{i=1}^{n_k-1} \sum_{j=i+1}^{n_k} p_{i,k} p_{j,k} d_{i,j,k}^2$$

553 We had CWV information for 18 traits for 1,099,463 plots, as at least two taxa were needed to  
554 calculate CWV. We performed the calculations using the 'data.table' package<sup>47</sup> in R.

555 **Vegetation trait-environment relationships.** Out of the 1,115,785 plots with CWM values,  
556 1,114,304 (99.9%) had complete environmental information and coordinates. This set of plots  
557 was used to calculate single linear regressions of each of the 18 traits on each of the 30  
558 environmental variables. We used the 'corrplot' function<sup>48</sup> in R to illustrate Pearson  
559 correlation coefficients (see Extended Data Figs. 1-2, 4, 6, 8) and for the strongest  
560 relationships produced bivariate graphs and mapped the global distribution of the CWM  
561 values using kriging interpolation in ArcGIS 10.2 (Fig. 3). We also tested for non-linear  
562 relationships with environment by including an additional quadratic term in the linear model  
563 and then report coefficients of determination. As in the linear relationships of CWM with  
564 environment, the highest  $r^2$  values in models with an additional quadratic term were  
565 encountered between stem specific density and PET ( $r^2=0.156$ ) and leaf N:P ratio and  
566 growing degree days above 5°C (GDD5,  $r^2=0.118$ ). These were not substantially different  
567 from the linear CWM-environment relationships, which had  $r^2=0.156$  and  $r^2=0.115$ ,  
568 respectively (Fig. 3, Extended Data Fig. 1). Similarly, including a quadratic term in the  
569 regressions did not increase the CWV-environment correlations. Here, the strongest  
570 correlations were encountered between plant height and soil pH ( $r^2=0.044$ ) and between  
571 specific leaf area (SLA) and the volumetric content of coarse fragments in the soil  
572 (CoarseFrag,  $r^2=0.037$ ), which were similar to those in the linear regressions ( $r^2=0.029$  and  
573  $r^2=0.036$ , respectively, Extended Data Fig. 2).

574 To account for a possible confounding effect of species richness on CWV, which may cause  
575 low CWV through competitive exclusion of species, we regressed CWV on species richness  
576 and then calculated all Pearson correlation coefficients with the residuals of this relationship



577 against all climatic variables. Here, the highest correlation coefficients were encountered  
578 between PET and CWV of conduit element length ( $r^2=0.038$ ), followed by the relationship of  
579 specific leaf area (SLA) and the volumetric content of coarse fragments in the soil  
580 (CoarseFrag,  $r^2=0.034$ ), which were very similar in magnitude to the CWV environment  
581 correlations ( $r^2=0.035$  and  $r^2=0.036$ , respectively; Extended Data Fig. 2).

582 The CWMs and CWVs were scaled to a mean of zero and standard deviation of one and then  
583 subjected to a Principal Component Analysis (PCA), calculated with the 'rda' function from  
584 the 'vegan' package<sup>49</sup>. Climate and soil variables were fitted *post hoc* to the ordination scores  
585 of plots of the first two axes, producing correlation vectors using the 'envfit' function. We  
586 refrain from presenting any inference statistics, as with > 1.1 million plots all environmental  
587 variables showed statistically significant correlations. Instead, we report coefficients of  
588 determination ( $r^2$ ), obtained from Redundancy Analysis (RDA), using all 30 environmental  
589 variables as constraining matrix, resulting in a maximum of 18 constrained axes  
590 corresponding to the 18 traits. We report both  $r^2$  values of the first two axes explained by  
591 environment, which is the maximum correlation of the best linear combination of  
592 environmental variables to explain the CWM or CWV plot  $\times$  trait matrix and  $r^2$  values of all  
593 18 constrained axes explained by environment. We plotted the PCA results using the 'ordiplot'  
594 function and coloured the points according to the logarithm of the number of plots that fell  
595 into grid cells of 0.002 in PCA units (resulting in approximately 100,000 cells). For further  
596 details, see the captions of the figures.

597 To analyse how plot-level trait means and within-plot trait variances depart from random  
598 expectation, for each trait we calculated standardized effect sizes (SESS) for the variance in  
599 CWM and SES for the mean in CWV. Significantly positive SESSs in variance of CWM and  
600 significantly negative ones in the mean of CWV can be considered a global-level measure of  
601 environmental filtering. To provide an indication of the global direction of filtering, we also  
602 report SESSs for the mean of CWM trait values. Similarly, to measure how much within-  
603 community trait dispersion varied globally, we also calculated SESSs for the variance in CWV.

604 SESSs were obtained from 100 runs of randomizing trait values across all species globally. In  
605 every run we calculated CWM and CWV with random trait values, but keeping all species  
606 abundances in plots. Thus, the results of randomization are independent from species co-  
607 occurrences structure of plots<sup>50</sup>. For every trait, the SESS of the variance in CWM, were  
608 calculated as the observed value of variance in CWM minus the mean variance in CWM of  
609 the random runs, divided by the standard deviation of the variance in CWM of the random  
610 runs. SESSs for the mean in CWM, the mean in CWV and the variance in CWV were  
611 calculated accordingly. Tests for significance of SESSs were obtained by fitting generalized  
612 Pareto-distribution of the most extreme random values and then estimating  $p$  values from this  
613 fitted distribution<sup>51</sup>.

614

615 **Testing for formation-specific patterns.** We carried out separate analyses for two  
616 'formations': forest and for non-forest plots. We defined as forest plots that had > 25% cover  
617 of the tree layer. However, this information was available for only 25% of the plots in our

618 sPlot database. Thus, we also assigned formation status based on growth form data from the  
619 TRY database. We defined plots as ‘forest’ if the sum of relative cover of all tree taxa was >  
620 25%, but only if this did not contradict the requirement of > 25% cover of the tree layer (for  
621 those records for which this information was given in the header file). Similarly, we defined  
622 non-forest plots by calculating the cover of all taxa that were not defined as trees and shrubs  
623 (also taken from the TRY plant growth form information) and that were not taller than 2 m,  
624 using the TRY data on mean plant height. We assigned the status ‘non-forest’ to all plots that  
625 had >90% cover of these low-stature, non-tree and non-shrub taxa. In total, 21,888 taxa out of  
626 the 52,032 in TRY which also occurred in sPlot belonged to this category, and 16,244 were  
627 classed as trees. The forests and non-forest plots comprised 330,873 (29.7%) and 513,035  
628 (46.0%) of all plots, respectively. We subjected all CWM values for forest and non-forest  
629 plots to PCA, RDA and bivariate linear regressions to environmental variables as described  
630 above.

631 The forest plots, in particular, confirmed the overall patterns, with respect to variation in  
632 CWM explained by the first two PCA axes (60.5%) and the two orthogonal continua from  
633 small to large size and the leaf economics spectrum (Extended Data Fig. 3). The variation  
634 explained by macroclimate and soil conditions was much larger for the forest subset than for  
635 the total data, with the best relationship (leaf N:P ratio and the mean temperature of the  
636 coldest quarter, bio11) having a  $r^2$  of 0.369 and the second next best ones (leaf N:P ratio and  
637 GDD1 and GDD5) close to this value with  $r^2=0.357$  (Extended Data Fig. 4) and an overall  
638 variation in CWM values explained by environment of 25.3% (cumulative variance of all 18  
639 constrained axes in a RDA). The non-forest plots showed the same functional continua, but  
640 with lower total amount of variation in CWM accounted for by the first two PCA axes  
641 (41.8%, Extended Data Fig. 5) and much lower overall variation explained by environment.  
642 For non-forests, the best correlation of any CWM trait with environment was the one of  
643 volumetric content of coarse fragments in the soil (CoarseFrag) and leaf C content per dry  
644 mass with  $r^2=0.042$  (Extended Data Fig. 6). Similarly, the cumulative variance of all 18  
645 constrained axes according to RDA was only 4.6%. This shows, on the one hand, that forest  
646 and non-forest vegetation are characterized by the same interrelationships of CWM traits, and  
647 on the other hand, that the relationships of CWM values with the environment were much  
648 stronger for forests than for non-forest formations. The coefficients of determination were  
649 even higher than those previously reported for trait-environment relationships for North  
650 American forests (between CWM of seed mass and maximum temperature,  $r^2=0.281$ )<sup>6</sup>.

651 **Resampling procedure in environmental space.** In order to achieve a more even  
652 representation of plots across the global climate space, we first subjected the same 30 global  
653 climate and soil variables as described above, to a Principal Component Analysis (PCA),  
654 using the climate space of the whole globe, irrespective of the presence of plots in this space,  
655 and scaling each variable to a mean of zero and a standard deviation of one. We used a 2.5 arc  
656 minute spatial grid, which comprised 8,384,404 terrestrial grid cells. We then counted the  
657 number of vegetation plots in the sPlot database that fell into each grid cell. For this analysis,  
658 we did not use the full set of 1,117,369 plots with trait information (see above), but only those  
659 plots that had a location inaccuracy of max. 3 km, resulting in a total of 799,400 plots. The  
660 resulting PCA scores based on the first two principal components (PC1-PC2) were rasterized

661 to a 100 × 100 grid in PC1-PC2 environmental space, which was the most appropriate  
662 resolution according to a sensitivity analysis. This sensitivity analysis tested different grid  
663 resolutions, from a coarse-resolution bivariate space of 100 grid cells (10 × 10) to a very fine-  
664 resolution space of 250,000 grid cells (500 × 500), iteratively increasing the number of cells  
665 along each principal component by 10 cells. For each iteration, we computed the total number  
666 of sPlot plots per environmental grid cell and plotted the median sampling effort (number of  
667 plots) across all grid cells versus the resolution of the PC1-PC2 space. We found that the  
668 curve flattens off at a bivariate environmental space of 100 × 100 grid cells, which was the  
669 resolution for which the median sampling effort stabilized at around 50 plots per grid cell. As  
670 a result, we resampled plots only in environmental cells with more than 50 plots (858 cells in  
671 total).

672 To optimize our resampling procedure within each grid cell, we used the heterogeneity-  
673 constrained random (HCR) resampling approach<sup>52</sup>. The HCR approach selects the subset of  
674 vegetation plots for which those plots are the most dissimilar in their species composition  
675 while avoiding selection of plots representing peculiar and rare communities that differ  
676 markedly from the main set of plant communities (outliers), thus providing a representative  
677 subset of plots from the resampled grid cell. We used the turnover component of the Jaccard's  
678 dissimilarity index ( $\beta_{jtu}$ <sup>53</sup>) as a measure of dissimilarity. The  $\beta_{jtu}$  index accounts for species  
679 replacement without being influenced by differences in species richness. Thus, it reduces the  
680 effects of any imbalances that may exist between different plots due to species richness. We  
681 applied the HCR approach within a given grid cell by running 1,000 iterations of randomly  
682 selecting 50 plots out of the total number of plots available within that grid cell. Where the  
683 cell contained 50 or fewer plots, all were included and the resampling procedure was not run.  
684 This procedure thinned out over-sampled climate types, while retaining the full environmental  
685 gradient.

686 All 1,000 random draws of a given grid cell were subsequently sorted according to the  
687 decreasing mean of  $\beta_{jtu}$  between pairs of vegetation plots and then sorted again according to  
688 the increasing variance in  $\beta_{jtu}$  between pairs of vegetation plots. Ranks from both sortings  
689 were summed for each random draw, and the random draw with the lowest summed rank was  
690 considered as the most representative of the focal grid cell. Because of the randomized nature  
691 of the HCR approach, this resampling procedure was repeated 100 times for each of the 858  
692 grid cells. This enabled us to produce 100 different subsamples out of the full sample of  
693 799,400 vegetation plots subjected to the resampling procedure. Each of these 100  
694 subsamples was finally subjected to ordinary linear regression, PCA and RDA as described  
695 above. We calculated the mean correlation coefficient across the 100 resampled data sets for  
696 each environmental variable with each trait.

697 To plot bivariate relationships, we used the mean intercept and slope of these relationships.  
698 PCA loadings of all 100 runs were stored and averaged. As different runs showed different  
699 orientation on the first PCA axes, we switched the signs of the axis loadings in some of the  
700 runs to make the 100 PCAs comparable to the reference PCA, based on the total data set.  
701 Across the 100 resampled data sets, we then calculated the minimum and maximum loading  
702 for each of the two PCA axes and plotted the result as ellipsoid. We also collected the post-  
703 hoc regressions coefficients of PCA scores with the environmental variables in each of the

704 100 runs, switched the signs accordingly and plotted the correlations to PC1 and PC2 as  
705 ellipsoids. The result is a synthetic PCA of all 100 runs. To illustrate the coverage of plots in  
706 PCA space, we used plot scores of one of the 100 random runs. Similarly, the coefficients of  
707 determination obtained from the RDAs of these 100 resampled sets were averaged.

708 The mean PCA loadings across these 100 subsets (summarized in Extended Data Fig. 7) were  
709 fully consistent with those of the full data set in Fig. 1, with the same two functional continua  
710 in plant size and diaspore mass (from bottom left to top right), and perpendicular to that, the  
711 leaf economics spectrum. The variation in CWM accounted for by the first two axes was on  
712 average  $50.9\% \pm 0.04$  standard deviations (SD), and thus, virtually identical with that in the  
713 total dataset. In contrast, the variation explained on average by macroclimate and soil  
714 conditions ( $26.5\% \pm 0.01$  SD as average cumulative variance of all 18 constrained axes in the  
715 RDAs across all 100 runs) was considerably larger than that for the total dataset, which is also  
716 reflected in consistently higher correlations between traits and environmental variables  
717 (Extended Data Fig. 8). The highest mean correlation was encountered for plant height and  
718 PET (mean  $r^2=0.342$  across 100 runs). PET was a better predictor for plant height than the  
719 precipitation of the wettest months (bio13, mean  $r^2=0.231$ ), as had been suggested  
720 previously<sup>7</sup>. The correlation of PET with stem specific density (mean  $r^2=0.284$ ) and warmth  
721 of the growing season (expressed as growing degree days above the threshold  $5^\circ\text{C}$ , GDD5)  
722 with leaf N:P ratio (mean  $r^2=0.250$ ) ranked among the best 12 correlations encountered out of  
723 all 540 trait-environment relationships, which confirms the patterns found in the whole data  
724 set (compared with Fig. 3). Overall, the coefficients of determination were much closer to the  
725 ones reported from other studies with a global collection of a few hundred plots ( $r^2$  values  
726 ranging from 36% to 53% based on multiple regressions of single traits with five to six  
727 environmental drivers<sup>22</sup>).

728

## 729 **References**

- 730 31. Boyle, B. *et al.* The Taxonomic Name Resolution Service: an online tool for automated  
731 standardization of plant names. *BMC Bioinformatics* **14**, 16 (2013).
- 732 32. Bremer, B. *et al.* An update of the Angiosperm Phylogeny Group classification for the  
733 orders and families of flowering plants: APG III. *Bot. J. Linn. Soc.* **161**, 105–121 (2009).
- 734 33. Schrodte, F. *et al.* BHPMF – a hierarchical Bayesian approach to gap-filling and trait  
735 prediction for macroecology and functional biogeography. *Global Ecol. Biogeogr.* **24**, 1510–  
736 1521 (2015).
- 737 34. Kattge J. *et al.* TRY—a global database of plant traits. *Glob. Change Biol.* **17**, 2905–2935  
738 (2011).
- 739 35. Shan, H. *et al.* Gap filling in the plant kingdom - Trait prediction using hierarchical  
740 probabilistic matrix factorization. *Proceedings of the 29<sup>th</sup> International Conference for*  
741 *Machine Learning (ICML 2012)* 1303–1310 (2012).

- 742 36. Fazayeli, F. *et al.* Uncertainty quantified matrix completion using Bayesian Hierarchical  
743 Matrix factorization. *13<sup>th</sup> International Conference on Machine Learning and Applications*  
744 (*ICMLA 2014*) 312–317 (2014).
- 745 37. Herz, K. *et al.* Drivers of intraspecific trait variation of grass and forb species in German  
746 meadows and pastures. *J. Veg. Sci.* **28**, 705–716 (2017).
- 747 38. Borgy, B. *et al.* Sensitivity of community-level trait–environment relationships to data  
748 representativeness: A test for functional biogeography. *Global Ecol. Biogeogr.* **26**, 729–739  
749 (2017).
- 750 39. Karger, D.N. *et al.* Climatologies at high resolution for the earth’s land surface areas. *Sci.*  
751 *Data* **4**, 170122. doi: 10.1038/sdata.2017.122 (2017)
- 752 40. Karger, D.N. *et al.* Climatologies at high resolution for the Earth land surface areas  
753 (Version 1.1). *World Data Center for Climate (WDCC) at DKRZ*. [http://chelsea-](http://chelsea-climate.org/downloads/)  
754 [climate.org/downloads/](http://chelsea-climate.org/downloads/) (2016).
- 755 41. Dee, D. P. *et al.* The ERA-Interim reanalysis: configuration and performance of the data  
756 assimilation system. *Q.J.R. Meteorol. Soc.* **137**, 553–597 (2011).
- 757 42. Synes, N.W. & Osborne, P.E. Choice of predictor variables as a source of uncertainty in  
758 continental-scale species distribution modelling under climate change. *Global Ecol. Biogeogr.*  
759 **20**, 904–914 (2011).
- 760 43. Enquist, B. *et al.* Scaling from traits to ecosystems: developing a general trait driver  
761 theory via integrating trait-based and metabolic scaling theories. *Adv. Ecol. Res.* **52**, 249–318  
762 (2015).
- 763 44. Buzzard, V. *et al.* Re-growing a tropical dry forest: functional plant trait composition and  
764 community assembly during succession. *Funct. Ecol.* **30**, 1006–1013 (2016).
- 765 45. Rao, C.R. Diversity and dissimilarity coefficients: A unified approach. *Theor. Popul. Biol.*  
766 **21**, 24–43 (1982).
- 767 46. Champely, S. & Chessel, D. Measuring biological diversity using Euclidean metrics.  
768 *Environ. Ecol. Stat.* **9**, 167–177 (2002).
- 769 47. Dowle, M. *et al.* data.table: Extension of Data.frame. R package version 1.9.6. (2015)  
770 <https://CRAN.R-project.org/package=data.table>
- 771 48. Friendly, M. Corrgrams: Exploratory displays for correlation matrices. *Am. Statistician*,  
772 **56**, 316–324 (2002).
- 773 49. Oksanen, J. *et al.* vegan: Community Ecology Package. R package version 2.3-3 (2016).  
774 <https://CRAN.R-project.org/package=vegan>
- 775 50. Hawkins, B.A. *et al.* Structural bias in aggregated species-level variables driven by  
776 repeated species co-occurrences: a pervasive problem in community and assemblage data. *J.*  
777 *Biogeogr.* **44**, 1199–1211 (2017).

- 778 51. Knijnenburg, T.A. *et al.* Fewer permutations, more accurate P-values. *Bioinformatics* **25**,  
779 i161–i168 (2009).
- 780 52. Lengyel, A., Chytrý, M. & Tichý, L. Heterogeneity-constrained random resampling of  
781 phytosociological databases. *J. Veg. Sci.* **22**, 175–183 (2011).
- 782 53. Baselga, A. The relationship between species replacement, dissimilarity derived from  
783 nestedness, and nestedness. *Global Ecol. Biogeogr.* **21**, 1223–1232 (2012).
- 784 54. Garnier, E. *et al.* Towards a thesaurus of plant characteristics: an ecological contribution.  
785 *J. Ecol.* **105**, 298–309 (2017). [www.top-thesaurus.org](http://www.top-thesaurus.org)

786

### 787 **Detailed Acknowledgements**

788 The study has been supported by the TRY initiative on plant traits (<http://www.try-db.org>).  
789 The TRY initiative and database is hosted, developed and maintained by J. Kattge and G.  
790 Bönisch (Max Planck Institute for Biogeochemistry, Jena, Germany). TRY is currently  
791 supported by DIVERSITAS/Future Earth and the German Centre for Integrative Biodiversity  
792 Research (iDiv) Halle-Jena-Leipzig.

793 Jan Altman was funded by research grants 17-07378S of the Grant Agency of the Czech  
794 Republic and long-term research development project no. RVO 67985939.

795 Isabelle Aubin was funded through Natural Sciences and Engineering Research Council of  
796 Canada and Ontario Ministry of Natural Resources and Forestry.

797 Idoia Biurrun was funded by the Basque Government (IT936-16).

798 Benjamin Blonder was supported by the UK Natural Environment Research Council  
799 (NE/M019160/1).

800 Anne Bjorkman and Isla Myers-Smith thank the Herschel Island-Qikiqtaruk Territorial Park  
801 management, Catherine Kennedy, Dorothy Cooley, Jill F. Johnstone, Cameron Eckert and  
802 Richard Gordon for establishing the ecological monitoring programme. Funding was provided  
803 by Herschel Island-Qikiqtaruk Territorial Park.

804 Zoltán Botta-Dukát was supported by project GINOP-2.3.2-15-2016-00019.

805 Andraž Čarni acknowledges the financial support from the Slovenian Research Agency  
806 (research core funding No. P1-0236).

807 Luis Cayuela was supported by project BIOCON08\_044 funded by Fundación BBVA.

808 Milan Chytrý and Ilona Knollová were supported by the Czech Science Foundation (14-  
809 36079G, Centre of Excellence Pladias).

810 Greg Guerin acknowledges support from the Terrestrial Ecosystem Research Network  
811 (Australia).

812 Alvaro G. Gutiérrez acknowledges FONDECYT 11150835, Project FORECOFUN-SSA

813 PIEF-GA-2010–274798), CONICYT-PAI (82130046).

814 Pedro Higuchi has been awarded a research grant by the Brazilian National Council for  
815 Scientific and Technological Development (CNPq).

816 Jürgen Homeier received funding from BMBF (Federal Ministry of Education and Science of  
817 Germany) and the German Research Foundation (DFG Ho3296-2, DFG Ho3296-4).

818 Jens Kattge acknowledges support by the Max Planck Institute for Biogeochemistry (Jena,  
819 Germany), Future Earth, the German Centre for Integrative Biodiversity Research (iDiv)  
820 Halle-Jena-Leipzig and the EU H2020 project BACI, Grant No 640176.

821 Jérôme Munzinger was supported by the French National Research Agency (ANR) with  
822 grants INC (ANR-07-BDIV-0008), BIONEOCAL (ANR-07-BDIV-0006) & ULTRABIO  
823 (ANR-07-BDIV-0010), by National Geographic Society (Grant 7579-04), and with fundings  
824 and authorizations of North and South Provinces of New Caledonia.

825 Ülo Niinemets and Meelis Pärtel were supported by the European Commission through the  
826 European Regional Development Fund (the Center of Excellence EcolChange). Meelis Pärtel  
827 acknowledges funding by the Estonian Ministry of Education and Research (IUT20-29)

828 Josep Peñuelas would like to acknowledge the financial support from the European Research  
829 Council Synergy grant ERC-SyG-2013-610028 IMBALANCE-P

830 Petr Petřík was supported by long-term research development project RVO 67985939 (The  
831 Czech Academy of Sciences).

832 Oliver Phillips is supported by an ERC Advanced Grant 29158 (“T-FORCES”) and is a Royal  
833 Society-Wolfson Research Merit Award holder.

834 Valério D. Pillar has been supported by the Brazil’s National Council of Scientific and  
835 Technological Development (CNPq, grant 307689/2014-0).

836 Peter B. Reich was supported by United States Department of Energy (DE-SL0012677), NSF  
837 grant IIS-1563950 and two University of Minnesota Institute on the Environment Discovery  
838 Grants.

839 Jens-Christian Svenning considers this work a contribution to his VILLUM Investigator  
840 project “Biodiversity Dynamics in a Changing World” funded by VILLUM FONDEN.

841 Cyrille Violle was supported by the European Research Council (ERC) Starting Grant Project  
842 "Ecophysiological and biophysical constraints on domestication of crop plants" (Grant ERC-  
843 StG-2014-639706-CONSTRAINTS) by the French Foundation for Research on Biodiversity  
844 (FRB; [www.fondationbiodiversite.fr](http://www.fondationbiodiversite.fr)) in the context of the CESAB project “Assembling,  
845 analysing and sharing data on plant functional diversity to understand the effects of  
846 biodiversity on ecosystem functioning: a case study with French Permanent Grasslands”  
847 (DIVGRASS).

848 Evan Weiher was funded by NSF DEB-0415383, UWEC-ORSP, and UWEC-BCDT.

849 We are indebted to Lukas Bruelheide for drawing the icons in Fig. 1 and 2. We would like to  
850 thank John Terborgh and Roel Brienem for contributing additional plot data.

851



852 Table 1: Traits used in this study and their function in the community. Traits are arranged  
 853 according to the degree to which they should respond to macroclimatic drivers.  $\updownarrow$  in the trait  
 854 column denotes reciprocal relationships,  $\updownarrow$  in the description column denotes trade-offs. For  
 855 trait units, plot-level trait means and within-plot trait variance see Extended Data Table 1.

Trait	Description	Function	Expected correlation with macroclimate
Specific leaf area, Leaf area, Leaf fresh mass, Leaf N, Leaf P $\updownarrow$	Leaf economics spectrum <sup>12-13,17</sup> : Thin, N-rich leaves with high turnover and high mass-based assimilation rates $\updownarrow$	Productivity, Competitive ability	Very high <sup>5-6,17,21,23</sup>
Leaf dry matter content, Leaf N per area, Leaf C	Thick, N-conservative, long-lived leaves with low mass-based assimilation rates		
Stem specific density	Fast growth $\updownarrow$ Mechanical support, Longevity	Productivity, Drought tolerance	Very high <sup>5,22</sup>
Conduit element length $\updownarrow$	Efficient water transport $\updownarrow$	Water use efficiency	High
Stem conduit density	Safe water transport		
Plant height	Mean individual height of adult plants	Competitive ability	High <sup>5,7</sup>
Seed number per reproductive unit $\updownarrow$	Seed economics spectrum <sup>23</sup> : Small, well dispersed seeds $\updownarrow$	Dispersal, Regeneration	Moderate <sup>23-24</sup>
Seed mass, Seed length, Dispersal unit length	Seeds with storage reserve to facilitate establishment and increase survival		
Leaf N:P ratio	P limitation (N:P > 15) N limitation (N:P < 10) <sup>28</sup>	Nutrient supply	Moderate <sup>29</sup>
Leaf nitrogen isotope ratio (leaf $\delta^{15}\text{N}$ )	Access to N derived from $\text{N}_2$ fixation $\updownarrow$ N supply via mycorrhiza	Nitrogen source, Soil depth	None

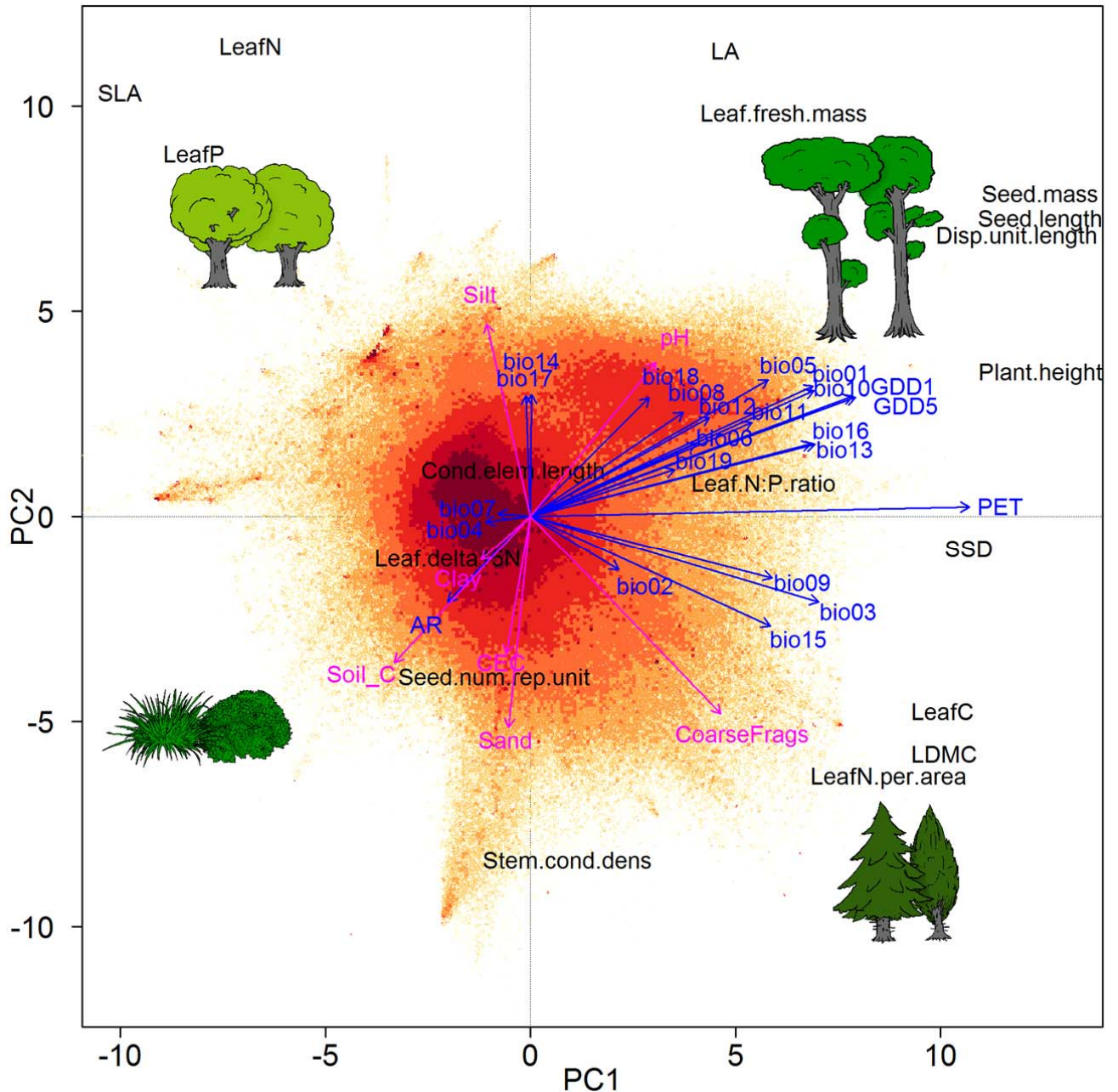
856

857

858 Fig. 1: Principal Component Analysis of global plot-level trait means (community-weighted  
 859 means, CWMs). The plots (n = 1,114,304) are shown by coloured dots, with shading  
 860 indicating plot density on a logarithmic scale, ranging from yellow with 1–4 plots at the same  
 861 position to dark red with 251–1142 plots. Prominent spikes are caused by a strong  
 862 representation of communities with extreme trait values, such as heathlands with ericoid  
 863 species with small leaf area and seed mass. Post-hoc correlations of PCA axes with climate  
 864 and soil variables are shown in blue and magenta, respectively. Arrows are enlarged in scale  
 865 to fit the size of the graph; thus, their lengths show only differences in variance explained  
 866 relative to each other. Variance in CWM explained by the first and second axis was 29.7%  
 867 and 20.1%, respectively. The vegetation sketches schematically illustrate the size continuum  
 868 (short vs. tall) and the leaf economics continuum (low vs. high LDMC and leaf N content per  
 869 area in light and dark green colours, respectively). See Extended Data Tables 1 and 2 for the  
 870 description of traits and environmental variables.

871

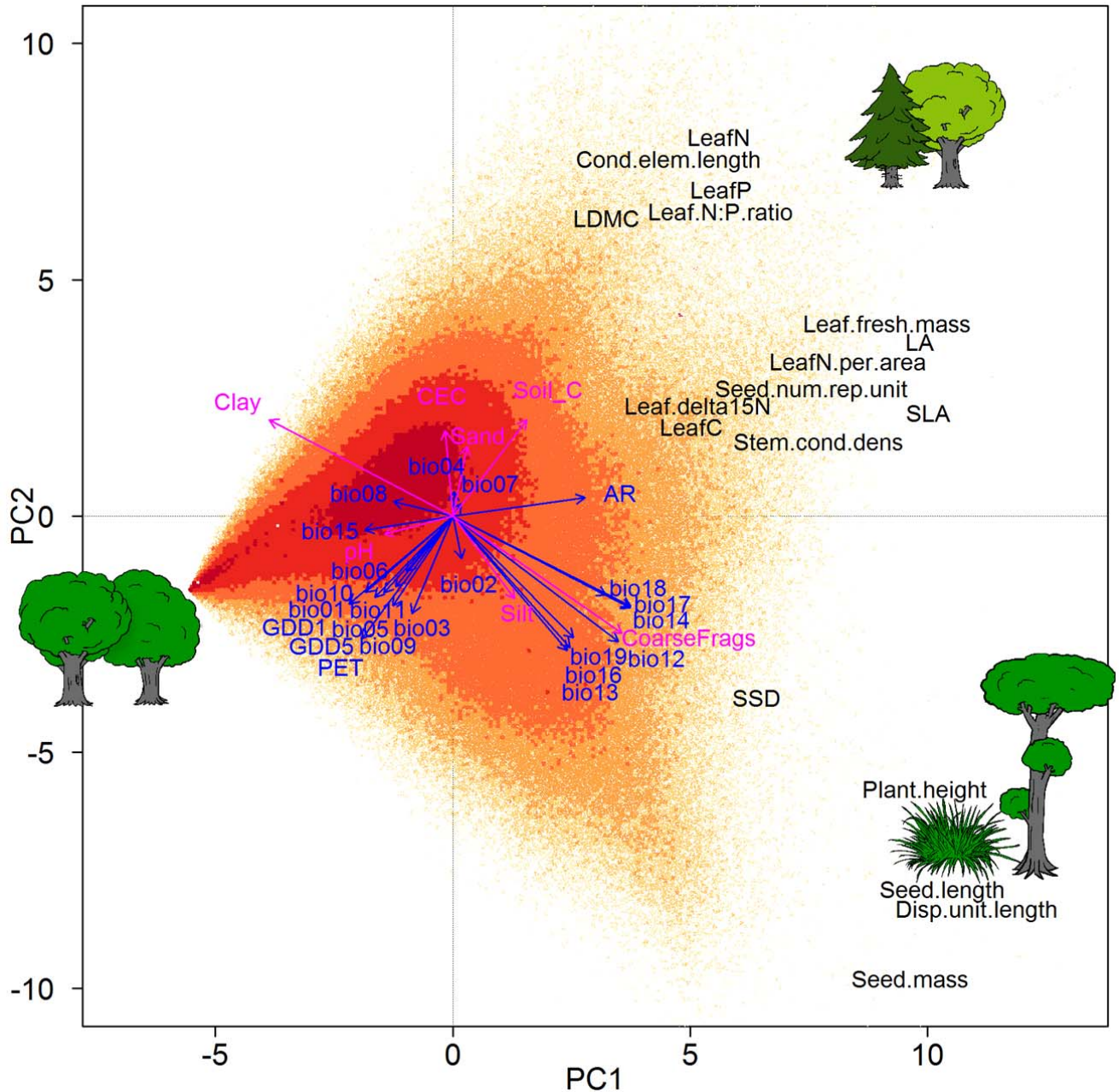
872



873 Fig. 2: Principal Component Analysis of global within-plot trait variances (community-  
 874 weighted variances, CWVs). The plots ( $n = 1,098,015$ ) are shown by coloured dots, with  
 875 shading indicating plot density on a logarithmic scale, ranging from yellow with 1–2 plots at  
 876 the same position to dark red with 631–1281 plots. Post-hoc correlations of PCA axes with  
 877 climate and soil variables are shown in blue and magenta, respectively. Arrows are enlarged  
 878 in scale to fit the size of the graph; thus, their lengths show only differences in variance  
 879 explained relative to each other. Variance in CWV explained by the first and second axis was  
 880 24.9% and 13.4%, respectively. CWV values of all traits increased from the left to the right,  
 881 which reflects increasing species richness ( $r^2 = 0.116$  between scores of the first axis and  
 882 number of species in the communities for which traits were available). The vegetation  
 883 sketches schematically illustrate low and high variation in the plant size and leaf economics  
 884 continua. See Extended Data Tables 1 and 2 for the description of traits and environmental  
 885 variables.

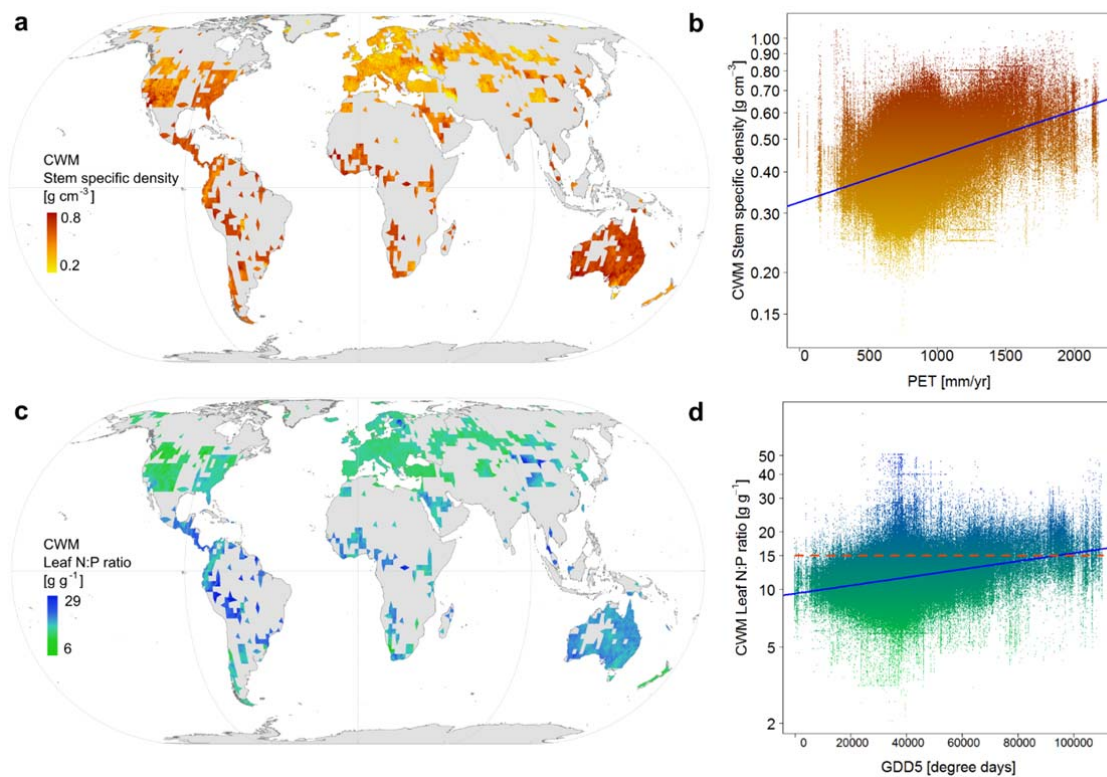
886

887



888 Fig. 3: The two strongest relationships found for global plot-level trait means (community-  
 889 weighted means, CWMs) in the sPlot dataset. CWM of the natural logarithm of stem specific  
 890 density [ $\text{g cm}^{-3}$ ] as a) global map, interpolated by kriging within a radius of 50 km around the  
 891 plots using a grid cell of 10 km, and b) function of potential evapotranspiration (PET,  
 892  $r^2=0.156$ ). CWM of the natural logarithm of the N:P ratio [ $\text{g g}^{-1}$ ] as c) global kriging map and  
 893 d) function of the warmth of the growing season, expressed as growing degree days over a  
 894 threshold of  $5^\circ\text{C}$  (GDD5,  $r^2=0.115$ ). Plots with N:P ratios  $> 15$  (of 2.71 on the  $\log_e$  scale) tend  
 895 to indicate phosphorus limitation<sup>28</sup> and are shown above the broken line in red colour (90,979  
 896 plots, 8.16% of all plots). The proportion of plots with N:P ratios  $> 15$  increases with GDD5  
 897 ( $r^2=0.895$  for a linear model on the log response ratio of counts of plots with N:P  $> 15$  and  
 898  $\leq 15$  counted within bins of 500 GDD5).

899



900

901

902 Extended Data Table 1: Traits, abbreviation of trait names, identifier in the Thesaurus Of Plant characteristics (TOP)<sup>54</sup>, units of measurement,  
903 observed values (obs.) standardized effect sizes (SES) and significance (p) of SES for means and variances of both plot-level trait means  
904 (community-weighted means, CWMs) and within-plot trait variances (community-weighted variances, CWVs). CWMs and CWVs were based on  
905 1,115,785 and 1,099,463 plots, respectively. All trait values were log<sub>e</sub>-transformed prior to analysis and observed and SES values are on the log<sub>e</sub>  
906 scale. Stem specific density is stem dry mass per stem fresh volume, specific leaf area is leaf area per leaf dry mass, leaf C, N and P are leaf carbon,  
907 nitrogen and phosphorus content, respectively, per leaf dry mass, leaf dry matter content is leaf dry mass per leaf fresh mass, leaf delta <sup>15</sup>N is the  
908 leaf nitrogen isotope ratio, stem conduit density is the number of vessels and tracheids per unit area in a cross section, conduit element length refers  
909 to both vessels and tracheids. SESs were calculated by randomizing trait values across all species globally 100 times and calculating CWM and  
910 CWV with random trait values, but keeping all species abundances in plots. Tests for significance of SES were obtained by fitting generalized  
911 Pareto-distribution of the most extreme random values and then estimating p values from this fitted distribution<sup>51</sup>. \* indicates significance at  $p <$   
912 0.05.

Trait	Abbreviation	TOP	Unit	CWM						CWV					
				mean			variance			mean			variance		
				obs.	SES	p	obs.	SES	p	obs.	SES	p	obs.	SES	p
Leaf area	LA	25	mm <sup>2</sup>	6.130	-9.75	*	1.691	12.53	*	1.565	-2.59	*	2.448	-0.27	n.s.
Specific leaf area	SLA	50	m <sup>2</sup> kg <sup>-1</sup>	2.850	9.89	*	0.172	12.88	*	0.150	-1.33	n.s.	0.023	1.10	n.s.
Leaf fresh mass	Leaf.fresh.mass	35	g	-2.125	-13.28	*	1.395	10.83	*	1.520	-2.05	*	2.311	0.01	n.s.
Leaf dry matter content	LDMC	45	g g <sup>-1</sup>	-1.294	-5.67	*	0.101	11.52	*	0.130	0.95	n.s.	0.017	6.73	*
Leaf C	LeafC	452	mg g <sup>-1</sup>	6.116	-3.77	*	0.003	8.80	*	0.002	-1.78	*	0.000	-0.38	n.s.
Leaf N	LeafN	462	mg g <sup>-1</sup>	3.038	4.22	*	0.055	6.29	*	0.063	-3.19	*	0.004	-0.13	n.s.
Leaf P	LeafP	463	mg g <sup>-1</sup>	0.535	9.57	*	0.097	2.81	*	0.117	-5.17	*	0.014	-2.11	*
Leaf N per area	LeafN.per.area	481	g m <sup>-2</sup>	0.251	-9.06	*	0.075	8.18	*	0.099	-0.28	n.s.	0.010	1.54	n.s.
Leaf N:P ratio	Leaf.N:P.ratio	-	g g <sup>-1</sup>	2.444	-11.95	*	0.040	0.40	n.s.	0.081	-2.74	*	0.007	-0.39	n.s.
Leaf δ <sup>15</sup> N	Leaf.delta15N	-	ppm	0.521	-3.58	*	0.254	6.68	*	0.455	2.82	*	0.207	2.44	*
Seed mass	Seed.mass	103	mg	0.407	-11.19	*	2.987	3.69	*	2.784	-9.06	*	7.750	-2.81	*
Seed length	Seed.length	91	mm	1.069	-4.51	*	0.294	5.50	*	0.365	-4.67	*	0.134	-3.07	*
Seed number per reproductive unit	Seed.num.rep.unit	-		6.179	7.67	*	2.783	4.40	*	5.156	1.44	n.s.	26.588	2.25	*
Dispersal unit length	Disp.unit.length	90	mm	1.225	-2.51	*	0.343	6.50	*	0.451	-3.21	*	0.203	-1.39	n.s.

Plant height	Plant.height	68	m	-0.315	-12.15	*	1.532	13.34	*	1.259	-9.01	*	1.585	9.68	*
Stem specific density	SSD	286	g cm <sup>-3</sup>	-0.869	-14.93	*	0.041	13.15	*	0.058	2.09	*	0.003	2.99	*
Stem conduit density	Stem.cond.dens	-	mm <sup>-2</sup>	4.407	15.08	*	0.656	8.45	*	0.975	-0.95	n.s.	0.951	1.10	n.s.
Conduit element length	Cond.elem.length	-	μm	5.946	-7.09	*	0.182	9.14	*	0.367	7.12	*	0.135	5.29	*
Mean SES					-3.50			8.06			-1.76			1.25	
Mean absolute SES					8.66			8.06			3.36			2.43	

913

914

915 Extended Data Table 2: Environmental variables used as predictors. Climate data were obtained from CHELSA<sup>38,39</sup> ([www.chelsa-climate.org](http://www.chelsa-climate.org)),  
 916 GDD1 and GDD5 were calculated from CHELSA data, based on monthly temperature and precipitation values for the years 1979–2013<sup>39-40</sup>. The  
 917 index of aridity (AR) and potential evapotranspiration (PET) were extracted from the CGIAR-CSI website ([www.cgiar-csi.org](http://www.cgiar-csi.org)). Soil variables were  
 918 obtained from the SOILGRIDS project (<https://soilgrids.org/>) and reflect mean values expected at 0.15 m depth.

919

Variable	Abbreviation	Unit	Data source
Annual Mean Temperature	Bio01	°C*10	CHELSA
Mean Diurnal Range (Mean of monthly (maximum temperature - minimum temperature))	Bio02	°C	CHELSA
Isothermality (bio2/bio7) (* 100)	Bio03	-	CHELSA
Temperature Seasonality (standard deviation of monthly temperature averages )	Bio04	°C*100	CHELSA
Max Temperature of Warmest Month	Bio05	°C*10	CHELSA
Min Temperature of Coldest Month	Bio06	°C*10	CHELSA
Temperature Annual Range (bio5-bio6)	Bio07	°C*10	CHELSA
Mean Temperature of Wettest Quarter	Bio08	°C*10	CHELSA
Mean Temperature of Driest Quarter	Bio09	°C*10	CHELSA
Mean Temperature of Warmest Quarter	bio10	°C*10	CHELSA
Mean Temperature of Coldest Quarter	bio11	°C*10	CHELSA
Annual Precipitation	bio12	mm/year	CHELSA
Precipitation of Wettest Month	bio13	mm/month	CHELSA
Precipitation of Driest Month	bio14	mm/month	CHELSA
Precipitation Seasonality	bio15	coefficient of variation	CHELSA
Precipitation of Wettest Quarter	bio16	mm/quarter	CHELSA
Precipitation of Driest Quarter	bio17	mm/quarter	CHELSA
Precipitation of Warmest Quarter	bio18	mm/quarter	CHELSA
Precipitation of Coldest Quarter	bio19	mm/quarter	CHELSA
Growing degree days above 1°C	GDD1	°C days	calculated
Growing degree days above 5°C	GDD5	°C days	calculated
Index of aridity	AR	(*10,000)	CGIAR-CSI

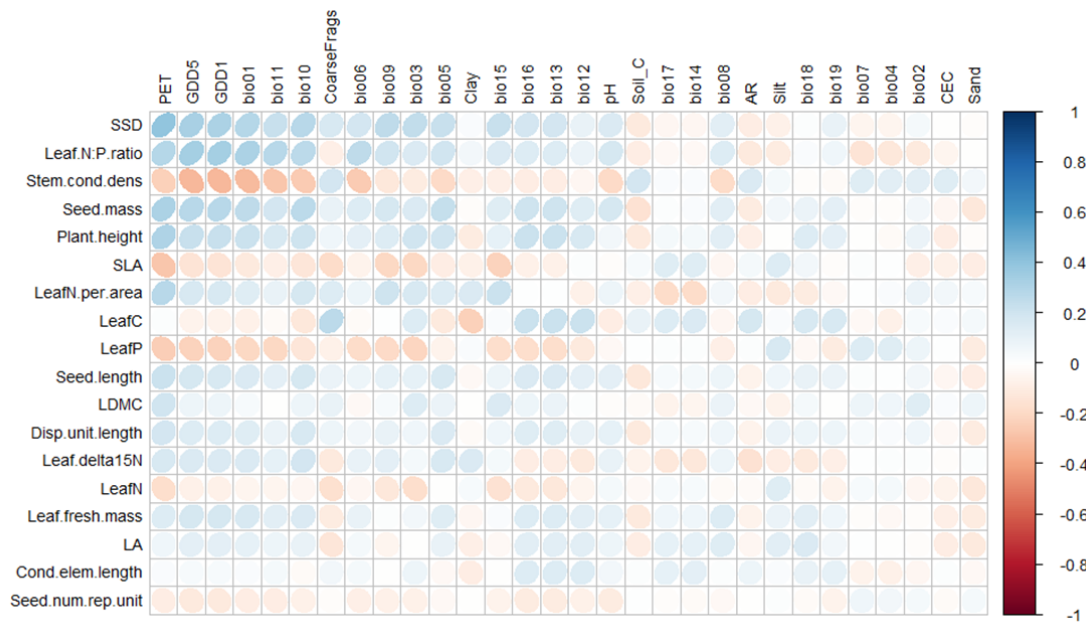
Potential evapotranspiration	PET	mm/year	CGIAR-CSI
Cation exchange capacity of soil	CEC	cmol <sub>c</sub> kg <sup>-1</sup>	SOILGRIDS
Soil pH	pH	(*10)	SOILGRIDS
Coarse fragment volume	CoarseFrag	vol. %	SOILGRIDS
Soil organic carbon content in the fine earth fraction	Soil_C	g kg <sup>-1</sup>	SOILGRIDS
Clay content (0–2 μm)	Clay	mass fraction %	SOILGRIDS
Silt content (2–50 μm)	Silt	mass fraction %	SOILGRIDS
Sand content (50–2000 μm)	Sand	mass fraction %	SOILGRIDS

920

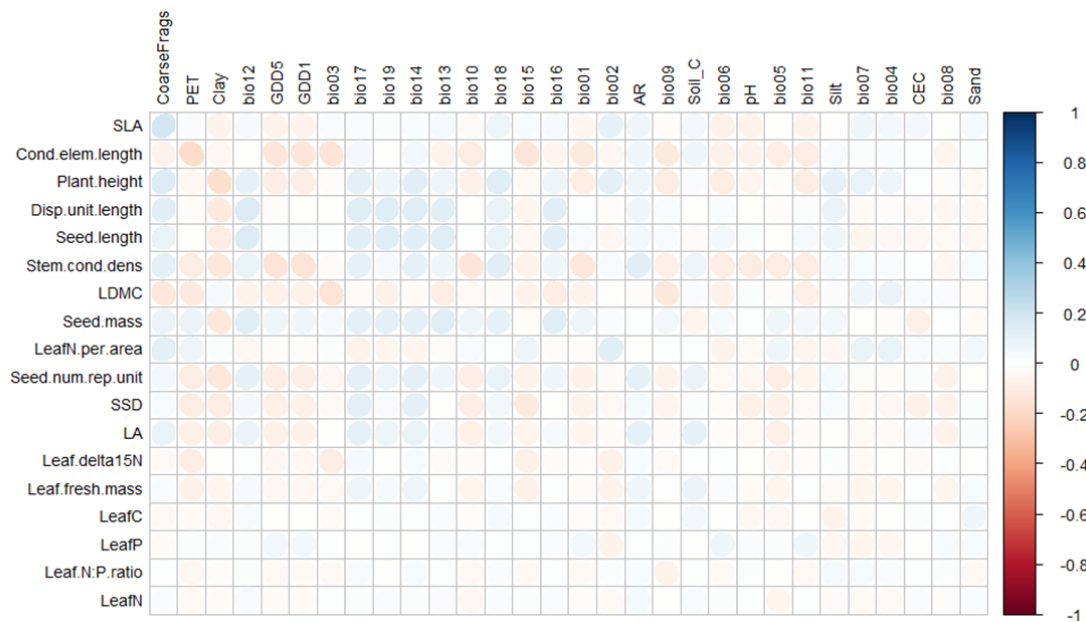
921



922 Extended Data Fig. 1: Visualisation of the Pearson correlation matrix of plot-level trait means  
 923 (community-weighted means, CWMs) of all 18 traits (rows) in the entire dataset (n =  
 924 1,114,304) with all 30 environmental predictors (columns). Positive correlations are shown in  
 925 blue, negative ones in red colour, with increasing colour intensity as the correlation value  
 926 moves away from 0. The eccentricity of the ellipses is scaled to the absolute value of the  
 927 correlation<sup>48</sup>. Rows and columns are arranged from top to bottom and from left to right  
 928 according to decreasing absolute correlation values. The highest correlation coefficient  
 929 (between stem specific density and PET) was 0.395 ( $r^2=0.156$ ). The best predictors for the  
 930 plant height and seed mass trade-off were potential evapotranspiration (PET) and growing  
 931 degree days above 5°C (GDD5), with  $r^2=0.093$  and 0.052 for plant height and  $r^2=0.099$  and  
 932 0.074 for seed mass, respectively. The best predictors for traits of the leaf economics  
 933 spectrum were PET and the seasonality in precipitation (bio15), with  $r^2=0.078$  and 0.051 for  
 934 specific leaf area (SLA) and  $r^2=0.039$  and 0.024 for leaf dry matter content (LDMC),  
 935 respectively. See Extended Data Tables 1 and 2 for the description of traits and environmental  
 936 variables.



938 Extended Data Fig. 2: Visualisation of the Pearson correlation matrix of within-plot trait  
 939 variances (community-weighted variances, CWVs) of all 18 traits (rows) in the entire dataset  
 940 ( $n = 1,098,015$ ) with all environmental predictors (columns). Positive correlations are shown  
 941 in blue, negative ones in red colour, with increasing colour intensity as the correlation value  
 942 moves away from 0. The eccentricity of the ellipses is scaled to the absolute value of the  
 943 correlation<sup>48</sup>. Rows and columns are arranged from top to bottom and from left to right  
 944 according to decreasing absolute correlation values. The highest correlation coefficient was  
 945 encountered between specific leaf area (SLA) and the volumetric content of coarse fragments  
 946 in the soil CoarseFrag,  $r^2=0.036$ ), followed by the correlation of PET to CWV of conduit  
 947 element length ( $r^2=0.035$ ). See Extended Data Tables 1 and 2 for the description of traits and  
 948 environmental variables.

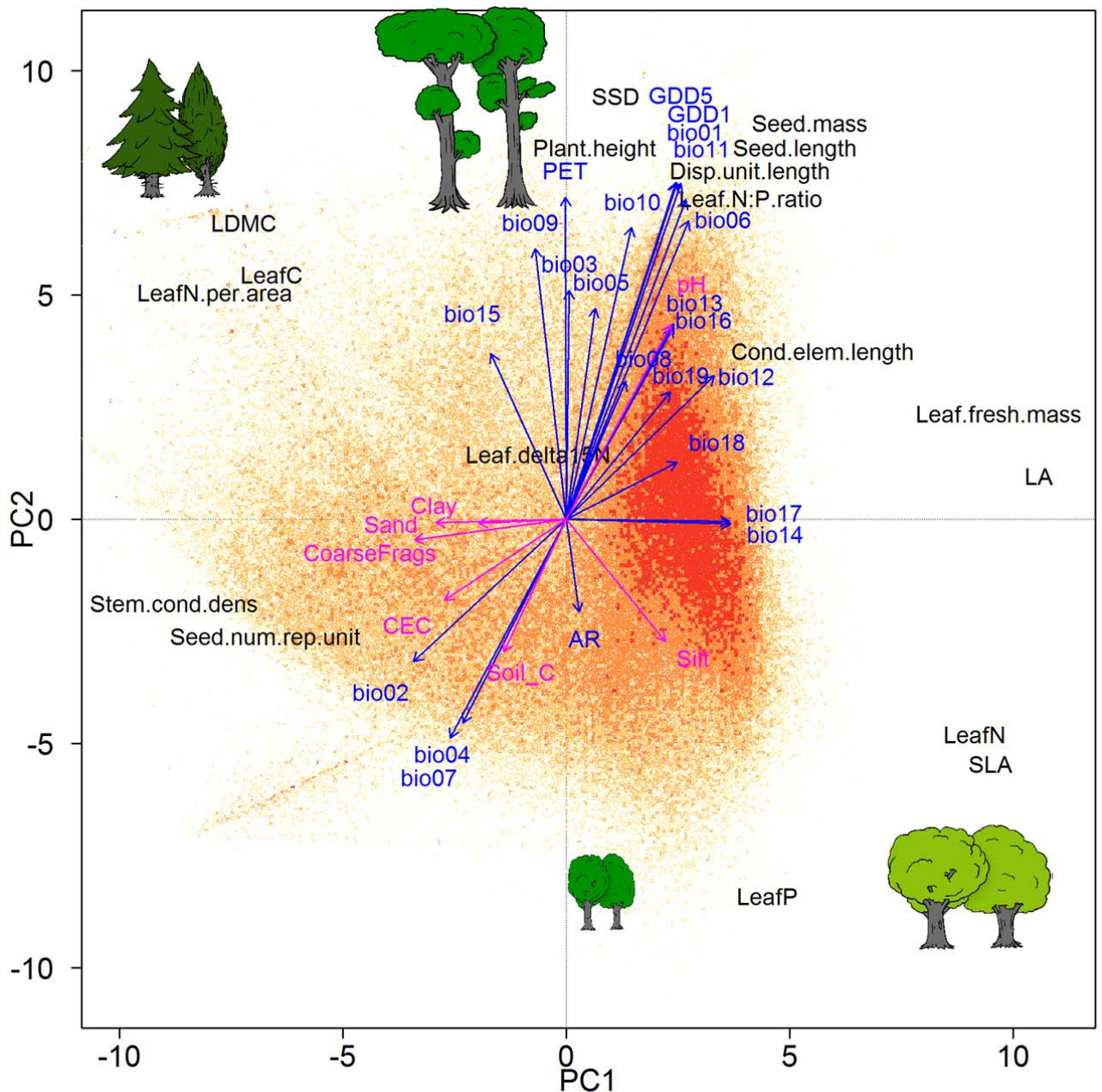


949

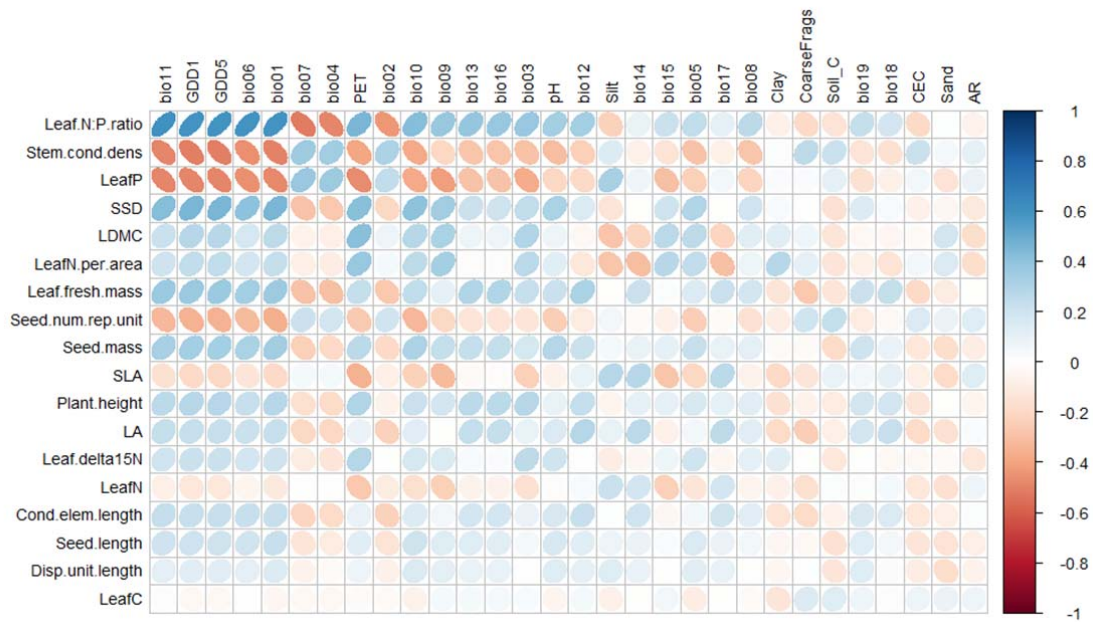
950

951 Extended Data Fig. 3: Principal Component Analysis of plot-level trait means (community-  
 952 weighted means, CWM) of forest communities only in the dataset. The plots (n = 330,873)  
 953 are shown by coloured dots, with shading indicating plot density on a logarithmic scale,  
 954 ranging from yellow with 1–4 plots at the same position to dark orange with 32–453 plots.  
 955 Post-hoc correlations of PCA axes with climate and soil variables are shown in blue and  
 956 magenta, respectively. Arrows are enlarged in scale to fit the size of the graph; thus, their  
 957 lengths show only differences in variance explained relative to each other. Variance in CWM  
 958 explained by the first and second axis was 32.9% and 27.6%, respectively. The vegetation  
 959 sketches schematically illustrate low and high variation in the plant size and leaf economics  
 960 continua. See Extended Data Tables 1 and 2 for the description of traits and environmental  
 961 variables.

962  
 963



964 Extended Data Fig. 4: Visualisation of the Pearson correlation matrix of plot-level trait means  
 965 (community-weighted means, CWMs) of all 18 traits (rows) of forest communities only in the  
 966 dataset ( $n = 330,873$ ) with all environmental predictors (columns). Positive correlations are  
 967 shown in blue, negative ones in red colour, with increasing colour intensity as the correlation  
 968 value moves away from 0. The eccentricity of the ellipses is scaled to the absolute value of  
 969 the correlation<sup>48</sup>. Rows and columns are arranged from top to bottom and from left to right  
 970 according to decreasing absolute correlation values. The highest correlation coefficient  
 971 (between leaf N:P ratio and the mean temperature of coldest quarter (bio11)) was 0.607  
 972 ( $r^2=0.369$ ). See Extended Data Tables 1 and 2 for the description of traits and environmental  
 973 variables.

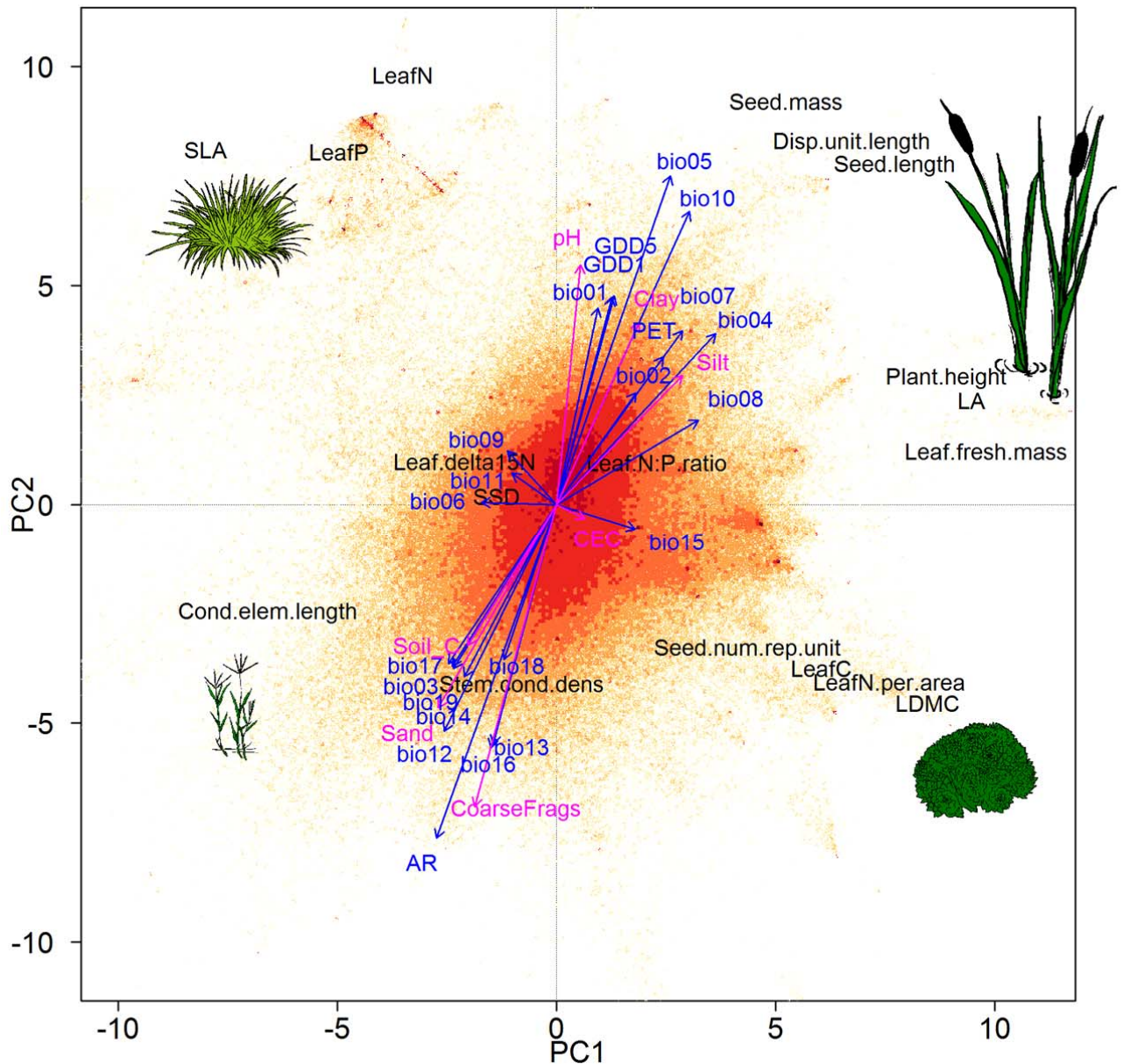


974

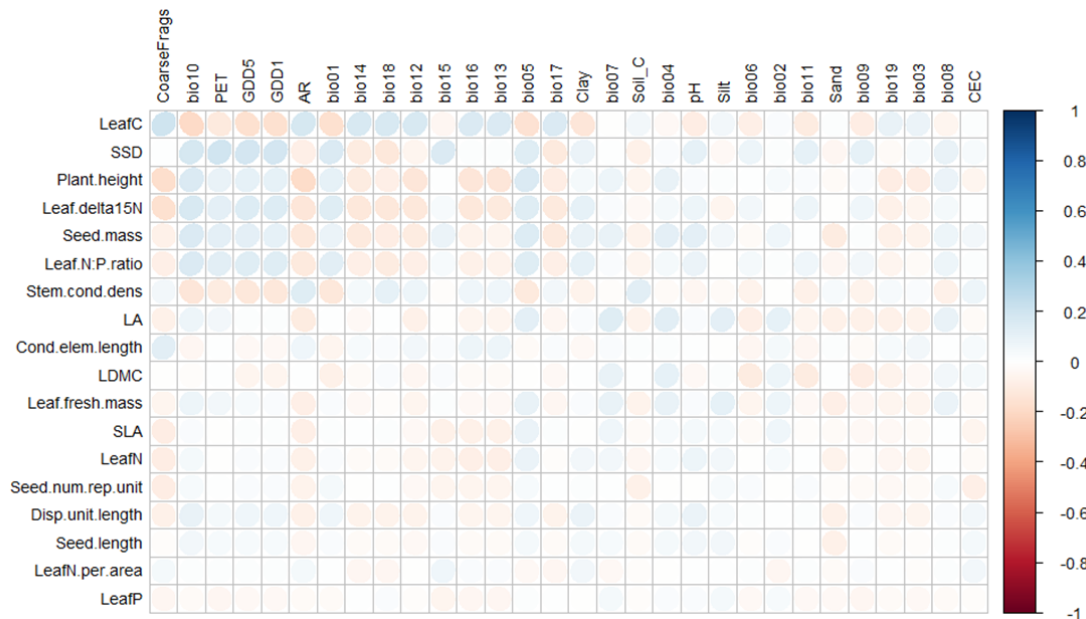
975

976 Extended Data Fig. 5: Principal Component Analysis of plot-level trait means (community-  
 977 weighted means, CWMs) of non-forest communities only in the dataset. The plots (n =  
 978 513,035) are shown by coloured dots, with shading indicating plot density on a logarithmic  
 979 scale, ranging from yellow with 1–4 plots at the same position to dark red with 251–1111  
 980 plots. Post-hoc correlations of PCA axes with climate and soil variables are shown in blue and  
 981 magenta, respectively. Arrows are enlarged in scale to fit the size of the graph; thus, their  
 982 lengths show only differences in variance explained relative to each other. Variance in CWM  
 983 explained by the first and second axis was 24.3% and 17.5%, respectively. The vegetation  
 984 sketches schematically illustrate low and high variation in the plant size and leaf economics  
 985 continua. See Extended Data Tables 1 and 2 for the description of traits and environmental  
 986 variables.

987  
 988



989 Extended Data Fig. 6: Visualisation of the Pearson correlation matrix of plot-level trait means  
 990 (community-weighted means, CWMs) of all 18 traits (rows) of non-forest communities only  
 991 in the dataset ( $n = 513,035$ ) with all environmental predictors (columns). Positive correlations  
 992 are shown in blue, negative ones in red colour, with increasing colour intensity as the  
 993 correlation value moves away from 0. The eccentricity of the ellipses is scaled to the absolute  
 994 value of the correlation<sup>48</sup>. Rows and columns are arranged from top to bottom and from left to  
 995 right according to decreasing absolute correlation values. The highest correlation coefficient  
 996 (between leaf C content per dry mass and the volumetric content of coarse fragments in the  
 997 soil (CoarseFragments)) was 0.204 ( $r^2=0.042$ ). See Extended Data Tables 1 and 2 for the  
 998 description of traits and environmental variables.

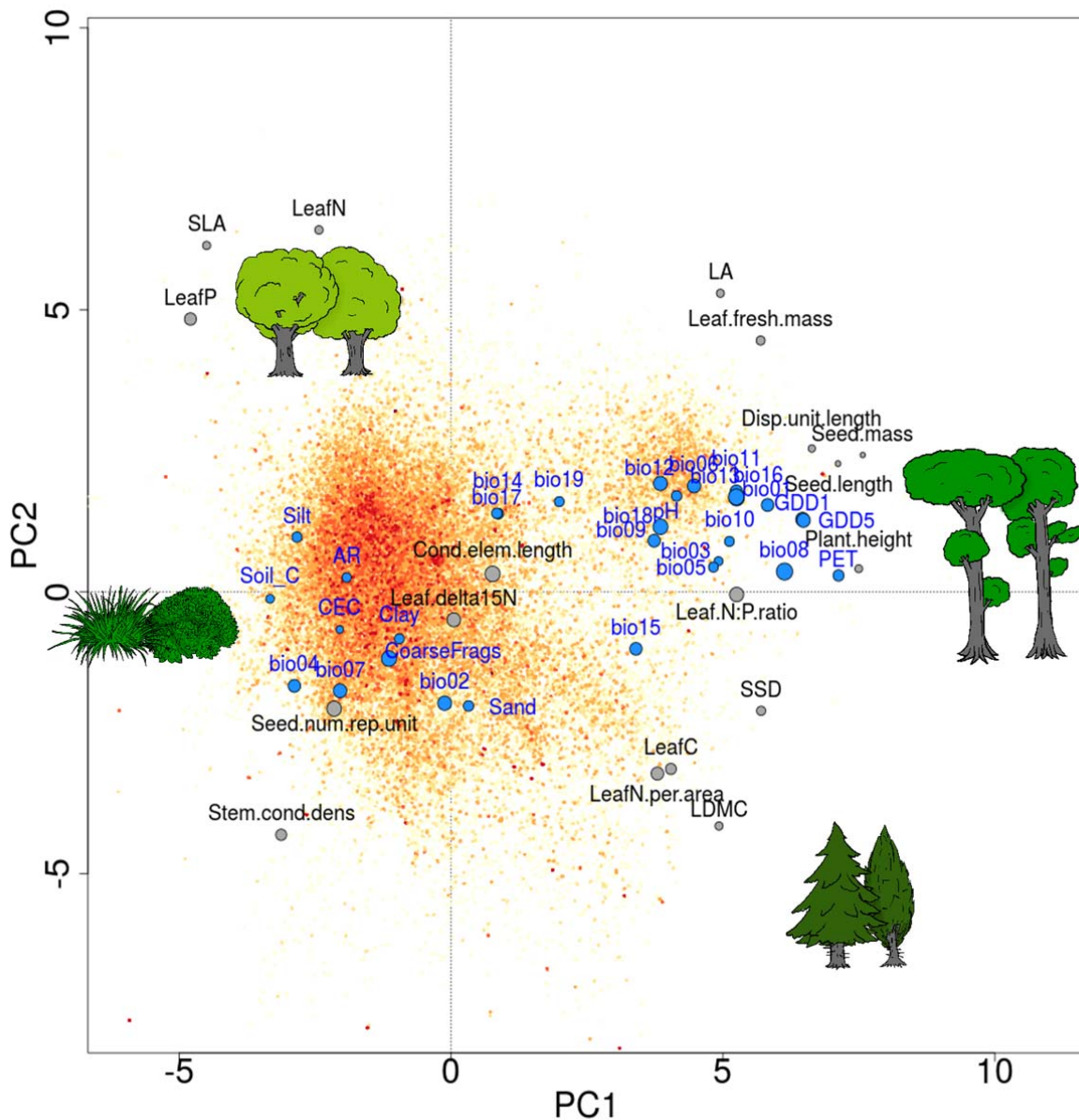


999

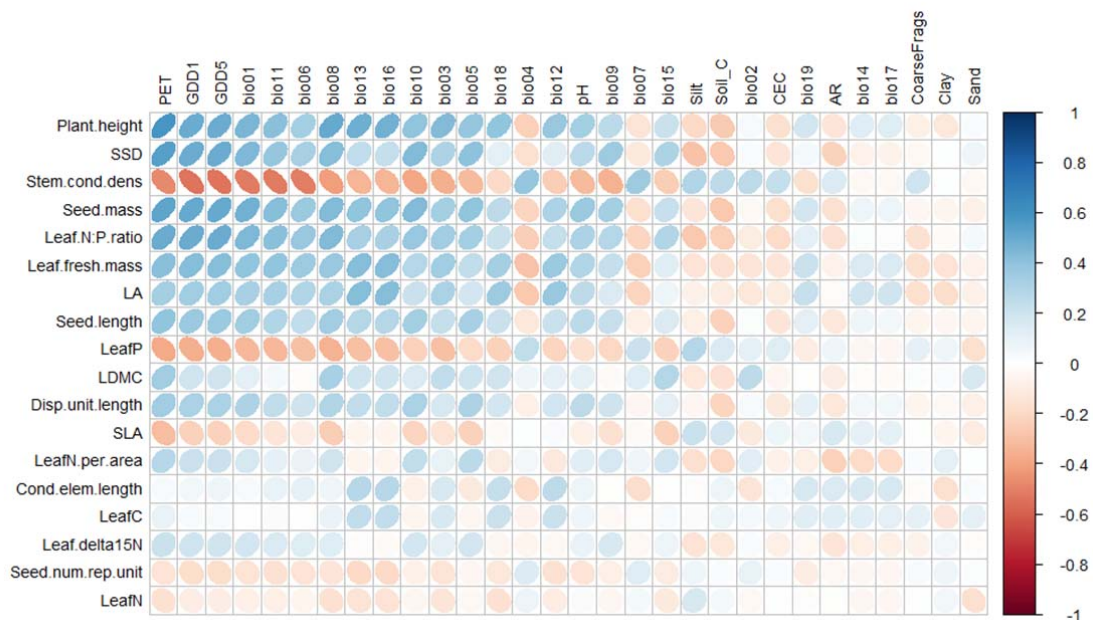
1000

1001 Extended Data Fig. 7: Summary of Principal Components Analyses applied to 100 resampled  
 1002 subsets of plot-level trait means (community-weighted means, CWMs) from the entire dataset  
 1003 for all 18 traits in the sPlot dataset. Each subset was resampled from the global environmental  
 1004 space (see Methods) and comprised between 99,342 and 99,400 (mean 99,380) plots. The  
 1005 coloured dots show the plots of one random example of these 100 subsets, with shading  
 1006 indicating plot density on a logarithmic scale, ranging from yellow with 1–3 plots at the same  
 1007 position to red with 10–81 plots in the subset. The loadings of each of the traits are displayed  
 1008 by a grey circle, its radius scaled to the range of loadings on PC1 and PC2 of all 100 runs.  
 1009 Post-hoc regressions of PCA axes with each of the environmental variables are illustrated by  
 1010 blue circles, its radius scaled to the range of correlations with PC1 and PC2.  
 1011 The circles are rather small, indicating that both the loadings and the post-hoc correlations with the  
 1012 environment had very similar values in the different runs. The mean variance in CWM  
 1013 explained by the first and second axis across the 100 runs was  $33.4\% \pm 0.04$  sd and  $17.5\% \pm$   
 1014  $0.03$  sd, respectively. The vegetation sketches schematically illustrate low and high variation  
 1015 in the plant size and leaf economics continua. See Extended Data Tables 1 and 2 for the  
 1016 description of traits and environmental variables.

1017



1018 Extended Data Fig. 8: Visualisation of the mean Pearson correlation coefficients of plot-level  
 1019 trait means (community-weighted means, CWMs) of all 18 traits (rows) with all  
 1020 environmental predictors (columns) of the 100 resampled subsets. Each subset was resampled  
 1021 from the global environmental space (see Methods) and comprised between 99,342 and  
 1022 99,400 (mean 99,379.5) plots. Positive correlations are shown in blue, negative ones in red  
 1023 colour, with increasing colour intensity as the correlation value moves away from 0. The  
 1024 eccentricity of the ellipses is scaled to the absolute value of the correlation<sup>48</sup>. Rows and  
 1025 columns are arranged from top to bottom and from left to right according to decreasing  
 1026 absolute mean correlation values. The highest mean correlation coefficient (between plant  
 1027 height and potential evapotranspiration (PET) was 0.585 ( $r^2=0.342$ ). See Extended Data  
 1028 Tables 1 and 2 for the description of traits and environmental variables.



1029  
 1030  
 1031